European Journal of Medicinal Chemistry 259 (2023) 115706

Contents lists available at ScienceDirect

European Journal of Medicinal Chemistry

journal homepage: www.elsevier.com/locate/ejmech

Research paper

Design, synthesis, and bioactivity evaluation of novel amide/sulfonamide derivatives as potential anti-inflammatory agents against acute lung injury and ulcerative colitis

Pan Chen [a,b,c,d,1], Jun Yang [b,1], Ying Zhou [b], Xiaobo Li [b], Yu Zou [b], Zhiwei Zheng [b], Mi Guo [b], Zhichao Chen [b], Won-Jea Cho [c], Nipon Chattipakorn [e], Wenqi Wu [b,d,**], Qidong Tang [b,d,*], Guang Liang [a,b,d,***]

[a] Department of Pharmacy and Institute of Inflammation, Zhejiang Provincial People's Hospital, Affiliated People's Hospital, Hangzhou Medical College, Hangzhou, 310014, China
[b] Chemical Biology Research Center, School of Pharmaceutical Sciences, Wenzhou Medical University, Wenzhou, 325035, China
[c] College of Pharmacy, Chonnam National University, Gwangju, 61186, Republic of Korea
[d] Wenzhou Institute, University of Chinese Academy of Sciences, Wenzhou, 325001, China
[e] Cardiac Electrophysiology Research and Training Center, Faculty of Medicine, Chiang Mai University, Chiang Mai, 50200, Thailand

ARTICLE INFO

Keywords:
Acute lung injury
Ulcerative colitis
Anti-inflammation
Amide/sulfonamide
NF-κB pathway

ABSTRACT

The uneven regulation of inflammation is related to various diseases, making anti-inflammation a potential option for the development of novel therapies. In this study, we designed and synthesized a total of fifty-eight novel amide/sulfonamide derivatives based on our previously reported anti-inflammatory compounds. The anti-inflammatory activities of these compounds were evaluated upon LPS-stimulated J774A.1 cells. Compounds **11a**, **11b**, **11c**, and **11d** potently reduced the release of IL-6 and TNF-α, and decreased the mRNA level of cytokines in J774A.1 cells. The most active compound **11d** with IC_{50} value of 0.61 μM for IL-6 inhibition, and 4.34 μM for TNF-α inhibition restored IκB α and inhibited the translocation of phosphorylated p65 into the nucleus. *In vivo* evaluation indicated that **11d** improved LPS-induced ALI and alleviated DSS-induced ulcerative colitis in mice. In conclusion, these results suggested compound **11d** can be a new lead structure for the development of anti-inflammatory drugs against ALI and ulcerative colitis.

1. Introduction

Inflammation is a normal immunological response that protects tissues from infections and heals the body after infection or trauma. Plenty of inflammatory mediators regulate inflammation. However, when the regulation becomes uneven or magnified, it can lead to a variety of illnesses including inflammatory bowel disease (IBD) and acute lung injury (ALI). As a result, regulating the immune system's release of inflammatory mediators and cytokines may be beneficial in the treatment of inflammatory illnesses [1].

ALI is a critical disease with a high mortality rate that occurs commonly in clinics [2]. Most symptoms of ALI being defined as a result of acute inflammation [3]. The main preventive treatment for ALI is mechanical ventilation [4]. Although various therapies have been studied (Table 1), they have shown limited effectiveness in reducing lung inflammation [5–9]. Interestingly, similar challenges exist in another non-specific inflammatory disease of the intestine called ulcerative colitis (UC), which has a globally increased incidence and prevalence ratio [10]. While aminosalicylates, corticosteroids, mesalazine, methotrexate, and immunomodulators are commonly used therapy options for UC, some patients exhibit inadequate responses or struggle with the associated adverse effects [11]. Therefore, it is evident that

* Corresponding author. Chemical Biology Research Center, School of Pharmaceutical Sciences, Wenzhou Medical University, Wenzhou, 325035, China.
** Corresponding author. Chemical Biology Research Center, School of Pharmaceutical Sciences, Wenzhou Medical University, Wenzhou, 325035, China.
*** Corresponding author. Department of Pharmacy and Institute of Inflammation, Zhejiang Provincial People's Hospital, Affiliated People's Hospital, Hangzhou Medical College, Hangzhou, 310014, China.
E-mail addresses: wenqiwu106@hotmail.com (W. Wu), tangqidongcn@126.com (Q. Tang), wzmcliangguang@163.com (G. Liang).
[1] These authors contribute equally to this work.

https://doi.org/10.1016/j.ejmech.2023.115706
Received 8 May 2023; Received in revised form 30 July 2023; Accepted 31 July 2023
Available online 2 August 2023

Table 1
Non-steroidal anti-inflammatory drugs treatment for ARDS in clinical trials.

Drugs	Target	Structure	Phase
Aspirin	COX-1/2		2
Celecoxib	COX-2	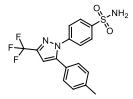	Unknown
Rosuvastatin	HMG-CoA	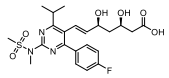	Unknown
Ibuprofen	COX-1/2	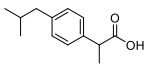	3
Simvastatin	HMG-CoA reductase	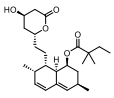	3
Losartan	angiotensin II	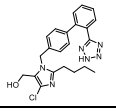	3

developing alternative strategies to tackle ALI and UC is crucial.

Many studies have found that cytokines have a role in the development of IBD [12,13] and ALI [14]. Interleukin-6 (IL-6) and tumor necrosis factor-α (TNF-α) contribute to most deterioration seen in ALI [15]. From human or experimental ALI studies, increased production of IL-6 and TNF-α has been found in the bronchoalveolar lavage fluid (BALF) [16]. Tumor necrosis factor (TNF) can cause the production of proinflammatory cytokines in colitis by connecting to its receptors and activating the transcription factor NF-κB. Other cytokines, such as IFN-α, IL-8, and IL-12, have been linked to the pathophysiology of IBD [17]. These reports indicate that inhibiting excessive production of pro-inflammatory cytokines, including IL-6 and TNF-α, can be a promising way for ALI and IBD treatment.

Sulfonamide structures play an important role in many natural products and medicines. Compounds containing the sulfonyl amide structure, such as compound **1** displayed in Fig. 1, showed significant anti-proliferation effects on non-small-cell lung carcinoma (NSCLC) [18] and melanoma cells [19]. Similarly, antibacterial compound **2** was found to serve as a specific inhibitor of CYP2C9 and to block the pro-inflammatory effects of linoleic acid mediated by CYP2C9 [20]. Moreover, some sulfa drugs work as anti-inflammatory [21], and antiviral [22] agents, such as compounds **3** and **4**, respectively. Taurine, compound **5**, is an amino acid available in mammals that contains a sulfonamide-like moiety [23]. Briefly, taurine works as a probe with endogenous antioxidant and anti-inflammatory capacities [24]. Moreover, Taurine has been reported to reduce the inflammatory response in ALI [25] and showed a beneficial effect in UC [26]. Previously, our research group has designed, synthesized, and evaluated some amide compounds inhibiting pro-inflammatory cytokines for the treatment of acute lung injury [27]. Amongst these compounds, *N*-(4-(4-hydroxy-3-methoxyphenyl) thiazol-2-yl)-3-(4-(3-nitrobenzyl) piperazin-1-yl) propanamide (compound **6**, Fig. 1) showed a potent inhibitory activity upon the production of inflammatory cytokines in a dose-dependent manner and displayed a protective effect against lipopolysaccharide (LPS)-induced ALI in a mice model. In order to find potent and patentable anti-inflammatory compounds for the treatment of ALI, we modified the 2-amino-4-phenylthiazole group of the compound **6** into pyridine or naphthalene rings and designed compounds **9a-9z**. Moreover, given the excellent potential of the sulfonamide structure in anti-inflammatory diseases, we herein performed the hybridization of compounds belonging to series **9** with taurine to deliver a new compound series **10**. Furthermore, we utilized scaffold hopping to replace the flexible alkyl chain with a phenyl group and synthesized compounds **11a-11g** to compare the anti-inflammatory activities between flexible chain and stiffness ring(Fig. 2). 2Figure 2. All synthesized compounds were evaluated for their anti-inflammatory effects in the context of LPS-induced production of IL-6 and TNF-α as well as for their structure-activity relationships. Subsequently, compounds **11a**, **11b**, **11c**, and **11d** were used for further *in vitro* investigation of their potential to reduce inflammatory cytokine production. Finally, we tested the protective effects of compound **11d** in an LPS-induced model of ALI and DSS-induced model of coliti.s.

2. Results

2.1. Chemistry

The synthetic route of amide/sulfonamide derivatives reported in this study was performed as illustrated in schemes 1, 3, and 4. Briefly, treatment of commercially available amine with various acetyl (propionyl), chloride, or sulfonyl chloride with triethyl amine provided the corresponding intermediates **7a-7k**. Then **7a-7k** were connected with different piperazine intermediates **8a-8f** or commercially available 2-(piperazin-1-yl) pyrimidine in the base condition with or without the catalyst of potassium iodide, resulting in the products **9a-9z**, **10a-10y** and **11a-11g**. The synthetic route of substituted piperazine intermediates **8a-8f** reported in this study was performed as depicted in Scheme 2 Excess piperazine was substituted by 4-nitrobenzene bromide or various substituted benzyl bromide, resulting in compounds **8a-e**. The thiozol-2-yl acetamide fragment **8f** was obtained from a *mannich* reaction of thizol-2-yl acetamide with *N*-Boc piperazine and paraformaldehyde, followed by removal of Boc group in trifluoro acetic acid. The structures of all synthesized compounds were fully characterized by ^{1}H nuclear magnetic resonance (NMR), ^{13}C NMR, and electrospray

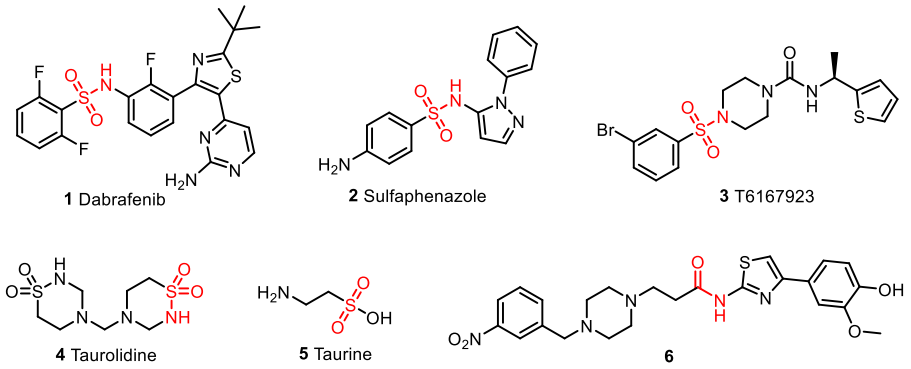

Fig. 1. Some structures of **amide/sulfonamide** compounds.

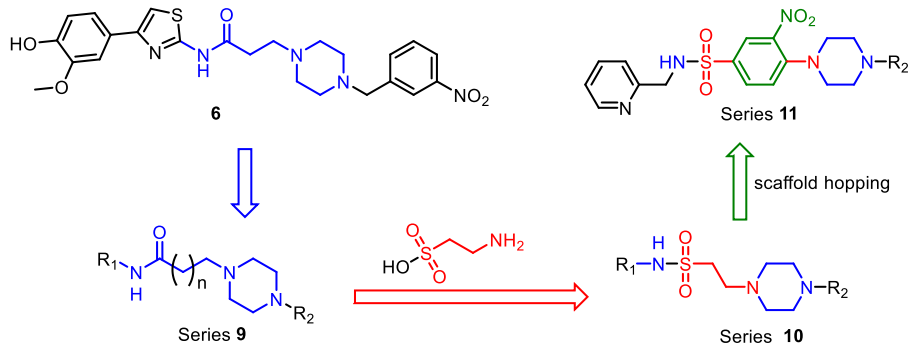

Fig. 2. Design strategy for the target compounds of amide/sulfonamide derivatives containing piperazine.

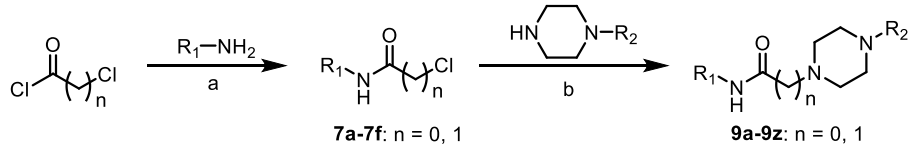

Scheme 1. (a) DCM, TEA, 0 °C to R.T.; (b) MeCN, K_2CO_3, 85 °C.

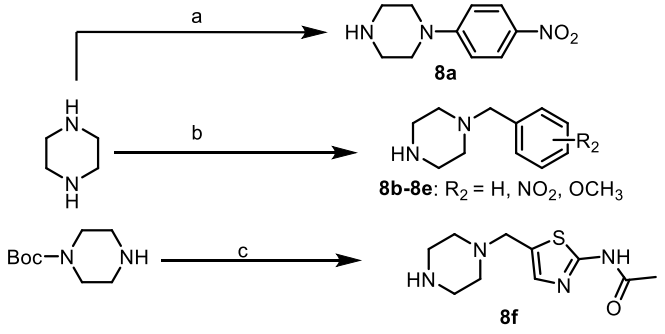

Scheme 2. (a) 4-nitrobenzene bromide, K_2CO_3, DMSO, 90 °C; (b) Different substituted benzyl bromide, DCM, 0 °C; (c) i. Paraformaldehyde, 2-Acetamidothiazole, acetic acid, 115 °C. ii. trifluoro acetic acid, R.T.

ionization mass spectrometry (ESI-MS), some active compounds were also characterized by high-resolution mass spectrometry (HRMS), together with the corresponding yield and melting points data, listed in the Experimental Section.

2.2. Initial anti-inflammatory screening against LPS-induced TNF-α and IL-6 release and primary study of structure-activity relationships (SAR)

To begin, we tested the synthesized compounds for anti-inflammatory activity. We used LPS to stimulate macrophages and induce the secretion of inflammatory factors, as described in our previous publications in *Eur. J. Med. Chem.*, *J. Med. Chem.*, and *Chem. Sci.* [15,28–31], and ELISA to measure the inhibitory effect of compound treatments on the aforementioned secretion of inflammatory factors. This approach has also been utilized for preliminary activity evaluation in other anti-inflammatory medication investigations published in *Eur. J. Med. Chem.* [32,33]. Briefly, J774A.1 cells were pretreated with 20 μM of synthesized compounds for 30 min, with compound **6** and DMSO serving as positive and negative controls, respectively. J774A.1 cells were then challenged with 0.5 μg/mL of LPS for 24 h. The amount of IL-6 and TNF-α in the medium was measured via ELISA kit according to the instructions provided by the manufacturer and normalized by the protein concentration of each sample. In addition, the cytotoxicity of compounds was evaluated using the MTT test on J774A.1 cells to rule out the possibility that the anti-inflammatory activity of the compounds was related to their cytotoxicity (Fig. S1).

To find potent and patentable anti-inflammatory compounds, series **9** compounds were designed by replacing the 2-amino-4-phenyl thiazole

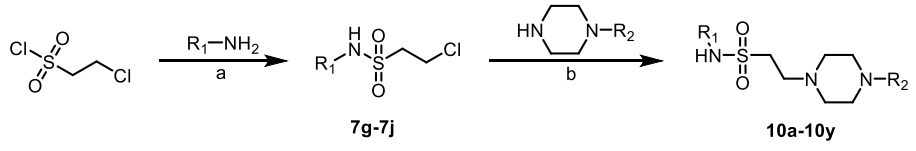

Scheme 3. (a) DCM, TEA, 0 °C to R.T.; (b) MeCN, K_2CO_3, 85 °C.

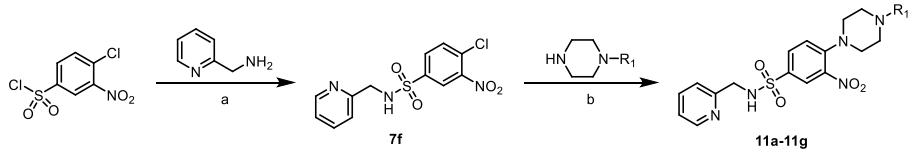

Scheme 4. (a) DCM, TEA, 0 °C to R.T.; (b) MeCN, K_2CO_3, KI, 85 °C.

moiety in compound **6** with a pyridine or naphthalene ring. Based on this, 26 compounds were synthesized (**9a-9z**) and their anti-inflammatory effects regarding the production of TNF-α and IL-6 upon LPS-challenged J774A.1 cells were investigated. As depicted in Table 2, compounds with 2-methoxypyridyl or 3-picolyl group or 1-naphthyl as R_1 showed moderate activity on the inhibition of IL-6 production when compared with compound **6**. Similarly, the inhibition of TNF-α production did not show a significant reduction after the abovementioned modification, with compounds **9d**, **9q,** and **9x** showing improved activity in the inhibition of TNF-α compared with compound **6**. 3-picolyl substituent as R_1 showed fairly increased activity on the inhibition of TNF-α production compared with 2-methoxypyridyl compounds and pyridyl compounds (**9d** vs **9m** and **9d** vs **9z**), 1-naphthyl group-containing compounds showed similar activity on the inhibition of TNF-α levels compared with 3-picolyl as R_1, which may indicate that there is a need for spatial distribution in these compounds to reduce the release of TNF-α. On the other hand, the IL-6 inhibition ratio increased when the nitro group was substituted at para-position rather than meta-position in the phenyl ring at R_2 (**9c** vs **9b**, **9m** vs **9l**, **9t** vs **9s**). Moreover, electron-withdrawing substitution in the phenyl ring at R_2 showed increased inhibition of TNF-α production compared with compounds that carried electron-donating substitution in the phenyl ring at R_2 (**9c** vs **9f**, **9m** vs **9p**, **9t** vs **9w**). These results revealed that the para-position substituted with electron withdrawing is preferred for the inhibition of TNF-α production.

Since the inhibition ratio of IL-6 and TNF-α did not reach the expected level, we performed the hybridization of series **9** compounds with taurine to modify the amide group into a sulfonyl amide group and designed series **10** in the following SAR studies (Table 3). Interestingly, it was found that this modification can potentially improve the anti-inflammatory activity of these molecules. Compounds with 3-picolyl as R_1 showed a markedly increased ratio in the inhibition of IL-6 production (**10a-10f** vs **9a-9f**). Similar to previous results, the para-position nitro substituent in the phenyl ring kept the anti-inflammatory activity better than that compounds with meta-position electron-withdrawing substituent (**10c** vs **10b**, **10i** vs **10h**, **10o** vs **10m**, **10v** vs **10u**). It was also found that compounds with a 6-quinolyl substituent showed a more robust effect on the production of IL-6 than 2-methoxypyrid-5-yl, 3-picolyl, and 1-naphthyl substituents compounds; however, **10t-10y** did not have a satisfying activity on the inhibition of TNF-α production (**10w** vs **10d**, **10j** and **10p**).

Given all the results we obtained until this point, we further utilized scaffold hopping to replace the flexible alkyl chain with a 3-nitrophenyl moiety and designed series **11** compounds. As depicted in Table 4, the inhibition ratio of IL-6 production instigated by compounds **11a-11d** dramatically increased (about 20–30%) after this modification, compared to that of compounds **10a-10d**. The substituent on the phenyl group in R_2 showed similar anti-inflammatory results to that of

Table 2
Relative inhibition of IL-6 and TNF-α production for series **9** compounds.

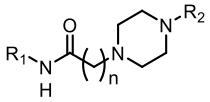

9a-9z

Index	R_1	n	R_2	IL-6 inhibition (%)[a]	TNF-α inhibition (%)
9a		1	benzyl	23.30 ± 4.19	40.91 ± 2.94
9b			3-nitrobenzyl	21.88 ± 1.82	39.82 ± 4.34
9c			4-nitrobenzyl	36.43 ± 10.32	42.80 ± 3.90
9d			4-nitrophenyl	49.31 ± 3.52	57.51 ± 4.29
9e			2-pyrimidyl	40.70 ± 0.57	38.32 ± 6.15
9f			4-methoxybenzyl	3.21 ± 16.09	38.64 ± 3.02
9g			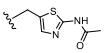	19.68 ± 5.28	36.32 ± 5.54
9h		2	benzyl	31.00 ± 1.21	40.52 ± 10.41
9i			4-nitrobenzyl	36.81 ± 10.26	25.79 ± 7.04
9j			4-nitrophenyl	19.64 ± 1.17	20.88 ± 3.62
9k		1	benzyl	9.69 ± 5.35	34.10 ± 8.31
9l			3-nitrobenzyl	20.88 ± 3.23	41.20 ± 5.03
9m			4-nitrobenzyl	35.43 ± 4.49	37.85 ± 2.53
9n			4-nitrophenyl	26.57 ± 2.67	35.31 ± 5.53
9o			2-pyrimidyl	33.21 ± 2.46	47.96 ± 2.73
9p			4-methoxybenzyl	19.35 ± 2.66	38.65 ± 3.35
9q			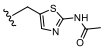	47.13 ± 5.20	53.08 ± 3.33
9r		1	benzyl	37.08 ± 1.88	40.65 ± 1.21
9s			3-nitrobenzyl	36.57 ± 1.07	49.62 ± 1.04
9t			4-nitrobenzyl	51.42 ± 1.21	44.12 ± 2.76
9u			4-nitrophenyl	17.67 ± 2.60	17.43 ± 1.54
9v			2-pyrimidyl	9.078 ± 4.07	18.50 ± 0.81
9w			4-methoxybenzyl	NA*	NA
9x		2	benzyl	50.93 ± 5.16	55.28 ± 7.36
9y			4-nitrophenyl	NA	NA
9z		1	4-nitrophenyl	54.40 ± 5.23	41.40 ± 4.05
6				78.47 ± 2.57	41.39 ± 0.97

*No activity.
a Values represented as mean ± SEM of at least three independent experiments.

Table 3
Relative inhibition of IL-6 and TNF-α production for series **10** compounds.

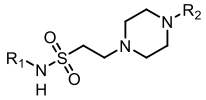

10a-10y

Index	R_1	R_2	IL-6 inhibition (%)[a]	TNF-α inhibition (%)
10a		benzyl	54.87 ± 4.29	43.92 ± 0.52
10b		3-nitrobenzyl	41.05 ± 2.67	38.96 ± 2.04
10c		4-nitrobenzyl	49.16 ± 3.87	41.37 ± 1.43
10d		4-nitrophenyl	60.10 ± 6.01	51.16 ± 0.88
10e		2-pyrimidyl	50.45 ± 1.84	40.39 ± 3.98
10f		4-methoxybenzyl	44.03 ± 2.36	35.94 ± 4.23
10g		benzyl	13.57 ± 4.48	16.24 ± 6.55
10h		3-nitrobenzyl	30.60 ± 2.82	34.88 ± 3.50
10i		4-nitrobenzyl	42.48 ± 4.30	38.83 ± 3.14
10j		4-nitrophenyl	54.03 ± 4.91	47.01 ± 1.14
10k		2-pyrimidyl	42.00 ± 5.51	37.77 ± 1.24
10l		4-methoxybenzyl	55.78 ± 4.70	39.86 ± 2.33
10m		benzyl	36.45 ± 5.63	38.58 ± 3.58
10n		3-nitrobenzyl	39.74 ± 1.42	48.04 ± 5.05
10o		4-nitrobenzyl	51.66 ± 2.86	52.22 ± 5.36
10p		4-nitrophenyl	54.08 ± 8.51	48.59 ± 1.90
10q		2-pyrimidyl	10.60 ± 4.56	12.33 ± 2.41
10r		4-methoxybenzyl	46.54 ± 3.65	38.07 ± 6.20
10s		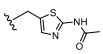	43.92 ± 2.39	25.56 ± 2.95
10t		benzyl	43.09 ± 0.97	9.54 ± 8.69
10u		3-nitrobenzyl	54.36 ± 2.33	23.97 ± 8.08
10v		4-nitrobenzyl	58.07 ± 1.35	24.49 ± 9.50
10w		4-nitrophenyl	63.27 ± 1.80	41.31 ± 6.18
10x		2-pyrimidyl	23.70 ± 3.22	5.34 ± 3.65
10y		4-methoxybenzyl	50.52 ± 2.83	31.97 ± 2.11

[a] Values represented as mean ± SEM of at least three independent experiments.

Table 4
Relative inhibition of IL-6 and TNF-α for series **11** compounds.

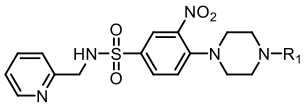

11a-11g

Index	R_1	IL-6 inhibition (%)[a]	TNF-α inhibition (%)
11a	benzyl	69.30 ± 0.53	50.22 ± 4.38
11b	3-nitrobenzyl	71.33 ± 1.53	43.51 ± 3.25
11c	4-nitrobenzyl	69.93 ± 2.35	42.19 ± 3.24
11d	4-nitrophenyl	85.92 ± 0.72	70.09 ± 1.91
11e	2-pyrimidyl	20.86 ± 3.85	18.24 ± 4.92
11f	4-methoxybenzyl	53.80 ± 4.49	18.06 ± 7.81
11g	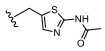	40.30 ± 2.01	31.13 ± 4.76

[a]Values are the mean of at least n = 3 independent experiments ± SEM.

compounds in series **9** and series **10**. In general, by conducting SAR studies, we had 3 novel series of anti-inflammatory compounds. Specifically, compounds **11b** and **11d** showed comparable inhibition of IL-6 production to that of compound **6,** and compounds **11a** and **11d** showed a better effect on the release of TNF-α compared to that of compound **6**, so we then used these four compounds in the next steps of our investigation.

2.3. Active compounds inhibited LPS-induced IL-6 and TNF-α release in a dose-dependent manner

The newly developed amide/sulfonamide derivatives showed exquisite SAR. To further explore the anti-inflammatory effect of active compounds, four of the most potent compounds **11a**, **11b**, **11c,** and **11d** were selected to investigate their dose-dependent inhibitory effects against LPS-induced IL-6 and TNF-α release. J774A.1 cells were pre-treated with selected compounds at indicated concentrations before the LPS challenge. As shown in Fig. 3A-3B, all active compounds exhibited a dose-dependent inhibition on the LPS-induced release of IL-6 and TNF-α. The IC_{50} values for compounds **11a**, **11b**, **11c,** and **11d** were found to be 4.94, 1.38, 1.32, and 0.61 μM for IL-6, and 10.09, 3.99, 8.59, and 4.34 μM for TNF-α, respectively. These results indicate that these compounds may be potential candidates for the development of anti-inflammatory agents.

2.4. Active compounds suppressed mRNA expressions in LPS-stimulated J774A.1 macrophages

To further determine the efficacy of active compounds on cytokine release, a real-time PCR assay was carried out to measure TNF-α and IL-6 mRNA levels in J774A.1 macrophages. Cells were challenged with LPS (0.5 μg/mL) for 6 h and examined for the expression of pro-inflammatory genes with or without **11a**, **11b**, **11c**, and **11d** treatment. As shown in Fig. 4A and B, mRNA levels of both IL-6 and TNF-α were upregulated following LPS incubation. While compounds **11a** and **11b** showed no significant effects on IL-6 mRNA levels, compounds **11c** and **11d** significantly downregulated mRNA levels of IL-6 and TNF-α. In

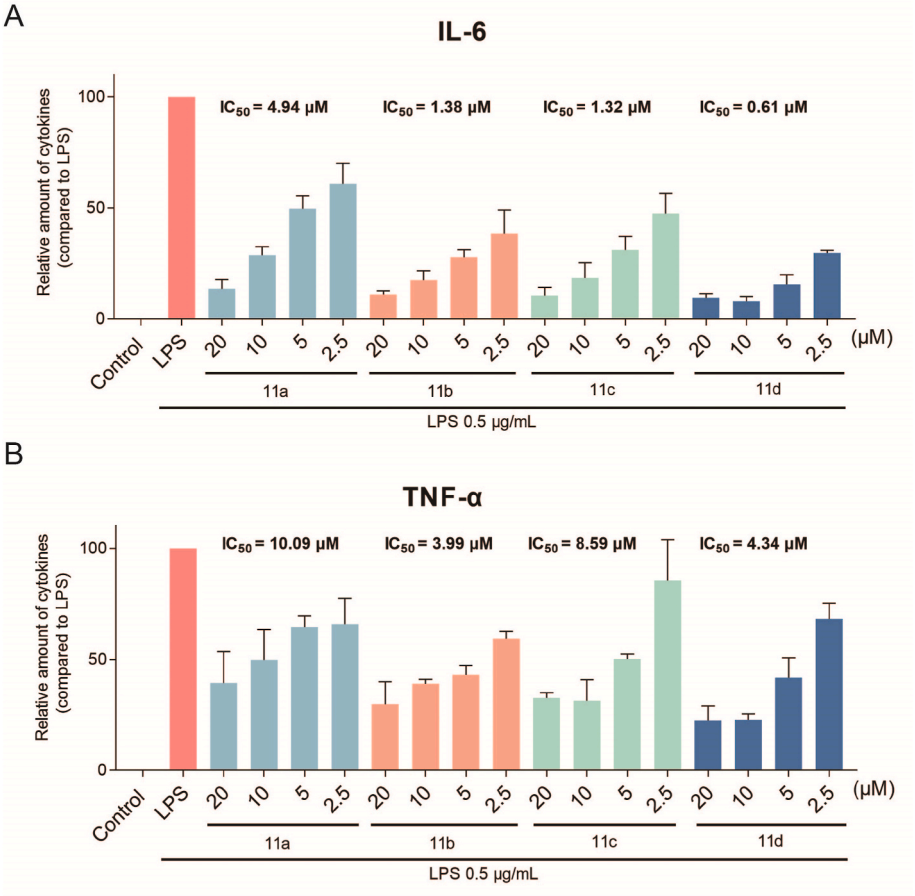

Fig. 3. Active compounds inhibiting LPS-induced inflammation cytokines release in J774A.1 cells. (A) IL-6 levels measured by ELISA. (B) TNF-α levels measured by ELISA. Each bar represents mean ± SEM in 3 independent experiments.

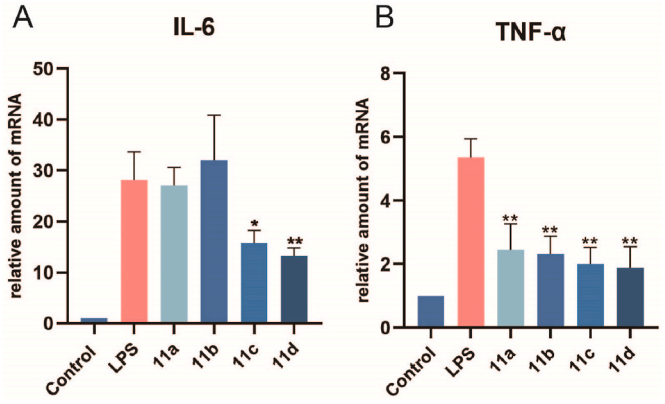

Fig. 4. Active compounds inhibit LPS-induced upregulation of mRNA levels of pro-inflammatory cytokines in J774A.1 cells. (A) IL-6 mRNA levels measured by qPCR. (B) TNF-α mRNA levels measured by qPCR. Data represented as mean ± SEM of three independent experiments. *, $p < 0.05$, **, $p < 0.01$ vs. the LPS-only group.

particular, **11d** showed the most active effect in inhibiting mRNA levels of tested inflammatory mediators. These data provided further evidence of the anti-inflammatory activity of compounds **11a**, **11b**, **11c,** and **11d**, which affect the cytokine profile at the mRNA level.

2.5. Active compound **11d** inhibited NF-κB pathway in J774A.1 cells

We next investigated the activity of compound **11d** on the modulation of nuclear factor kappa-light-chain-enhancer of activated B cells (NF-κB) pathway. This pathway plays an important role in the regulation of inflammatory response. After LPS stimulation, p65 is phosphorylated and transferred into the cell nucleus, which is followed by the expression of cytokines and chemokines that contribute to the inflammatory response. J774A.1 cells were pretreated with compound **11d** at 20 μM for 2 h before the challenge with 0.5 mg/mL LPS. Then macrophages were fixed and stained with an antibody against p65 and 4,6-diamidino-2-phenylindole (DAPI) via an immunofluorescence assay. As shown in Fig. 5A and B, the levels of p65 in the cell nucleus were significantly increased in cells treated with LPS only when compared with counterparts in the control group. Conversely, pretreatment with compound **11d** markedly reduced the levels of p65 translocated into the nucleus. Western blotting results indicated that the levels of IκB α, one of the most common members of the NF-κB pathway, were reduced and the levels of phosphorylated p65 (p-p65) were increased in the nucleus after the LPS challenge. Pretreatment with compound **11d** restored IκB α protein levels to baseline and downregulated the levels of p-p65 in the nucleus (Fig. 5C–E and Fig. S2). These results revealed that the anti-inflammatory activity of **11d** may be mediated via the inhibition of the NF-κB pathway.

2.6. Protective effects of **11d** on a mice model of LPS-induced ALI

Encouraged by its potent *in vitro* anti-inflammatory activity,

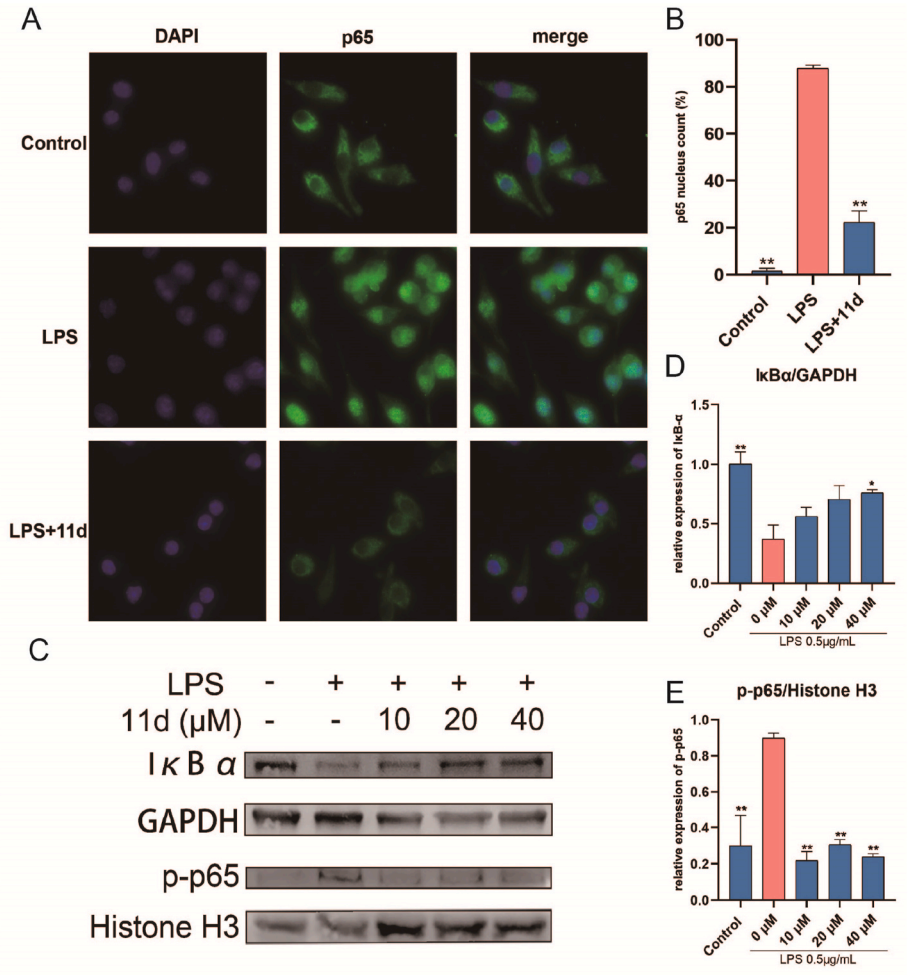

Fig. 5. Compound **11d** pretreatment inhibited the NF-κB pathway to reduce the inflammatory tone. (A) Representative picture of immunofluorescence results of J774A.1 cells treated with compound **11d**. DAPI staining is shown in blue and the immunofluorescence results of p65 are shown in green. (B) Quantification of results shown in A. Each bar represents the mean ± SEM in 3 independent experiments. *, $p < 0.05$, vs. the LPS-only group. (C) Western blotting results regarding the actions of compound **11d** on the NF-κB pathway. (D, E) Densitometric quantification of IκB-α, and p-p65. Each bar represents the mean ± SEM in 3 independent experiments. *, $p < 0.05$, **, $p < 0.01$ vs. the LPS-only group.

compound **11d** was selected for further investigation on its effects *in vivo* in a mouse model of LPS-induced ALI. C57BL/6 mice were pretreated with compound **11d** at 20 mg/kg for 30 min by intragastric administration. Then, 5 mg/kg of LPS was used to induce ALI in mice by intratracheal injection. The serum, BALF, and lung tissues were collected for further analysis. The lung wet/dry weight ratio was used as an index of lung edema. As shown in Fig. 6A, the lung wet/dry weight ratio increased after LPS administration when compared with the control group. Strikingly, pretreatment with compound **11d** at 20 mg/kg significantly decreased the lung wet/dry ratio, indicating that **11d** inhibits LPS-induced lung edema. The protein concentration in BALF is another important indicator of the structural integrity of the alveolar wall. It markedly increased after LPS stimulation whereas pretreatment with compound **11d** significantly reduced the protein concentration in BALF (Fig. 6B). In addition, the histopathological features of lung tissue in ALI mice after exposure to LPS were tested. As shown in Fig. 6C, when compared to the control group, the LPS group remarkably increase the alveolar septa thickness, pulmonary congestion, inflammatory infiltration, and lung tissue destruction. Moreover, and importantly, the lung tissue of mice pretreated with compound **11d** displayed little to no histopathological changes. Altogether, these results indicate that **11d** effectively attenuates LPS-induced ALI in mice.

Pro-inflammatory cytokines are critical factors in ALI progression. As such, the production levels of TNF-α and IL-6 in the BALF and sera of LPS-induced ALI mice were examined as biomarkers for the *in vivo* protection effects of compound **11d** on ALI. The release of TNF-α and IL-6 in the BALF and serum were significantly increased after LPS stimulation. In contrast, pretreatment with compound **11d** distinctly suppressed the levels of both cytokines, demonstrating that this compound is able to markedly attenuate inflammation in ALI mice (Fig. 7A–D). Interestingly, the mRNA expression of pro-inflammatory cytokines of LPS-challenged lung tissues significantly increased (Fig. 7E and F), whereas pretreatment with compound **11d** led to a decrease of TNF-α and IL-6 mRNA levels. These data revealed that compound **11d** improves ALI therapy via its anti-inflammatory effects and could potentially be used for treating ALI.

2.7. Effect of compound *11d* on DSS-induced colitis

The effect of **11d** on colitis was then tested on a DSS-induced acute colitis mouse model. DSS refers to a frequently-used inducer of colitis, due to the morphology and symptoms of DSS-induced colitis being similar to human ulcerative colitis [34]. 2.5% DSS in water was given for the 7 days. **11d** was administered orally to mice at a dose of 5 mg/kg every day for 10 days. At the end of the experimental treatment, the colon and spleen of each mouse were removed and measured, the serum was collected for cytokines measurement. The results are shown in Fig. 8. DSS significantly decrease the colonic length, while **11d** restored the colon lengths of UC mice (Fig. 8A and Fig. S3). The spleen/weight results indicated that **11d** reduced the splenomegaly induced by DSS (Fig. 8B). The IL-6 level also markedly decreased after the treatment of **11d** (Fig. 8C). The histopathological analysis showed severe pathological changes in the DSS-induced model, including mucosal damage, crypt necrosis, and infiltration of inflammatory cells in the lamina propria (Fig. 8D). **11d** ameliorated these symptoms and showed protective effects against DSS-induced colitis. The spleen tissues in the DSS group revealed an increase in the white pulp, which may indicate the hyperactivation of the spleen. **11d** treatment significantly attenuated the increase of white pulp. Taken together, these results indicated that compound **11d** can alleviate the severity of DSS-induced ulcerative colitis in the mouse.

2.8. Pharmacokinetic properties and tissue distribution of *11d*

Based on the favorable anti-inflammatory activity of **11d** *in vitro* and *in vivo*, the pharmacokinetics of **11d** were then evaluated following intravenous injection and oral administration in rats, respectively. Compound **11d** showed favorable pharmacokinetic properties after a single 10 mg/kg dose, with an AUC value of 1057.5 h*ng/mL and a t1/2 value of 7.1 h (Table 5). The oral bioavailability of **11d** is 10.6%, and the maximum plasma levels were reached at around 2.8 h.

3. Conclusion

In summary, we designed and synthesized fifty-eight amide/

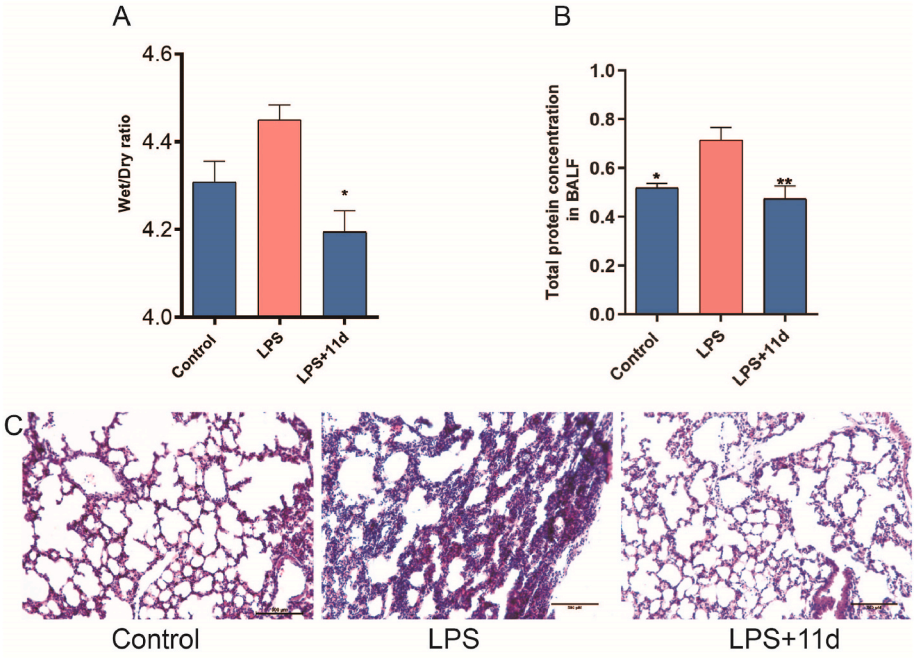

Fig. 6. Protective effects of compound **11d** in a mouse model of LPS-induced ALI. (A) Lung wet/dry ratio. (B) Total protein concentration in BALF. (C) Hematoxylin and eosin (H&E) staining results of lung tissue (200 ×). Data presented as mean ± SEM, n = 8, *, $p < 0.05$, **, $p < 0.01$ vs. the LPS-only group.

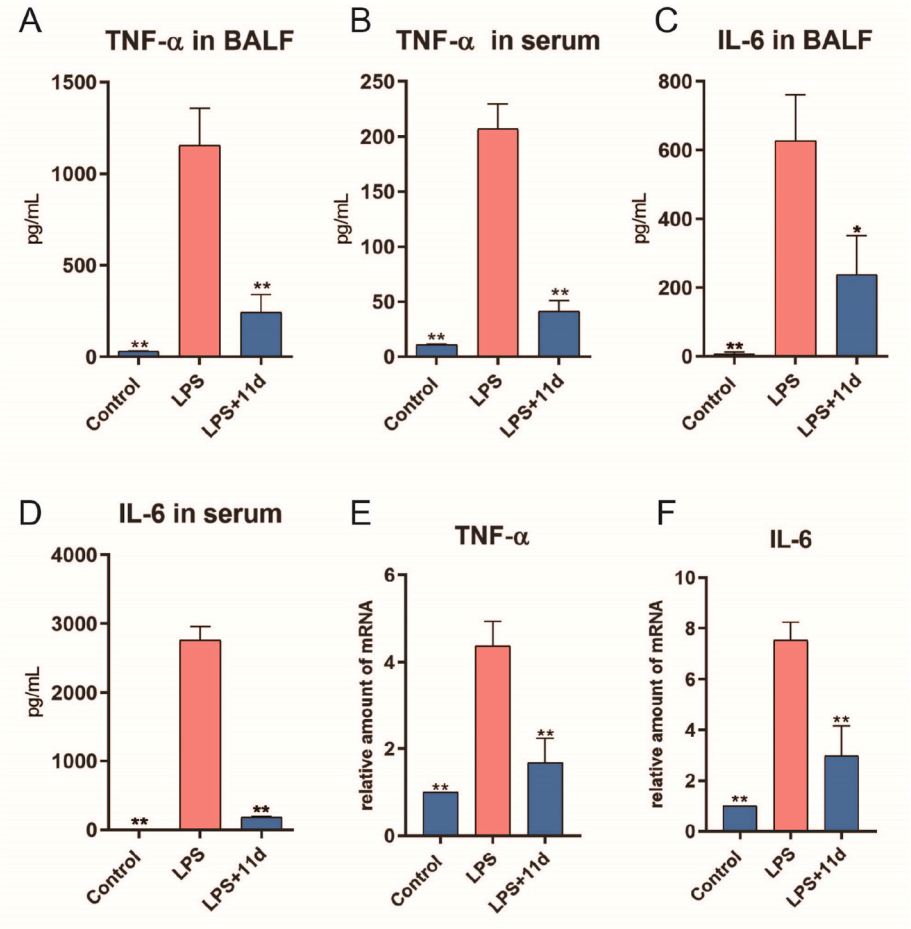

Fig. 7. Attenuation of acute LPS-induced pulmonary inflammation by compound **11d**. (A) TNF-αlevels in BALF measured by ELISA. (B) IL-6 levels in BALF measured by ELISA. (C) TNF-α levels in serum measured by ELISA. (D) IL-6 levels in serum measured by ELISA. (E) mRNA levels of TNF-α in lung tissue measured by qPCR. (F) mRNA levels of IL-6 in lung tissue measured by qPCR. Data presented as mean ± SEM, n = 8, *, $p < 0.05$, **, $p < 0.01$ vs. the LPS-only group.

sulfonamide derivatives and evaluated their anti-inflammatory activity upon the LPS challenge of J774A.1 cells. Most of the resulting compounds effectively inhibited the production of TNF-α and IL-6 in macrophages. In particular, compounds **11a, 11b, 11c,** and **11d** showed a dose-dependent inhibition on the release of TNF-α and IL-6 and reduced the mRNA levels of two cytokines *in vitro*. Moreover, **11d** inhibited the translocation of p65 into the nucleus and restored the IκBα level after the LPS stimulation on J774A.1 cells. Furthermore, pretreatment with **11d** attenuated LPS-induced ALI in mice via reducing the lung W/D ratio, macrophage infiltration into lung tissue, and the production of cytokines in BALF and serum. Moreover, **11d** also alleviated DSS-induced ulcerative colitis in mice. Overall, these results suggested compound **11d** could be utilized as an anti-inflammatory agent for the treatment of some inflammatory diseases and this work provides new lead structures for the development of anti-inflammatory drugs.

4. Experiment section

4.1. Chemistry

4.1.1. General

All reagents and solvents of analytical grade were obtained from commercial sources and used without further purification. All reactions were monitored by thin-layer chromatography (250 silica gel 60 F_{254} glass plates). Chromatographic purification was carried out on silica gel (200–300 mesh). ^{1}H and ^{13}C NMR spectra were recorded using a Bruker Avance III HD400 FT-NMR spectrometer, using tetramethylsilane as an internal standard. Electronspray ionization mass spectra in positive mode (ESI-MS) results were collected on Xevo TQ-S micro instrument and SCIEX TripleTOF 6600 system. The purity of compounds was determined by high-performance liquid chromatography (HPLC) to a percentage above 95%, monitored by UV absorption at 210 and 254 nm.

4.1.2. General procedure for preparation of intermediates ***7a-7k***

To a solution of primary amine and triethylamine in DCM at 0 °C it was added acetyl (propionyl) chloride or sulfonyl chloride in dropwise. After warming the resulting mixture at RT for 16 h, it was diluted with water and the aqueous layer was extracted with DCM (3 × 20 mL). The combined organic extracts were dried with anhydrous Na_2SO_4, filtered, and concentrated under reduced pressure. The crude material was purified by chromatography on silica (10–100% EtOAc in hexanes) to obtain intermediates **7a-7k**.

4.1.3. 2-Chloro-N-(pyridin-2-ylmethyl)acetamide (*7a*)

Brown oil in 67.69% yield; ^{1}H NMR (400 MHz, DMSO-d_6) δ 8.81 (d, J = 6.1 Hz, 1H), 8.51 (dd, J = 4.9, 1.4 Hz, 1H), 7.77 (td, J = 7.7, 1.8 Hz, 1H), 7.32–7.23 (m, 2H), 4.41 (d, J = 5.9 Hz, 2H), 4.18 (s, 2H).

4.1.4. N-(pyridin-2-ylmethyl)acrylamide (*7b*)

Yellow oil in 69.26% yield; ^{1}H NMR (400 MHz, DMSO-d_6) δ 8.74–8.58 (m, 1H), 8.50 (tdd, J = 3.8, 1.8, 1.0 Hz, 1H), 7.76 (td, J = 7.7, 1.7 Hz, 1H), 7.34–7.23 (m, 2H), 6.34 (dd, J = 17.1, 10.2 Hz, 1H), 6.13 (dd, J = 17.1, 2.1 Hz, 1H), 5.64 (dd, J = 10.2, 2.2 Hz, 1H), 4.44 (d, J = 6.0 Hz, 1H).

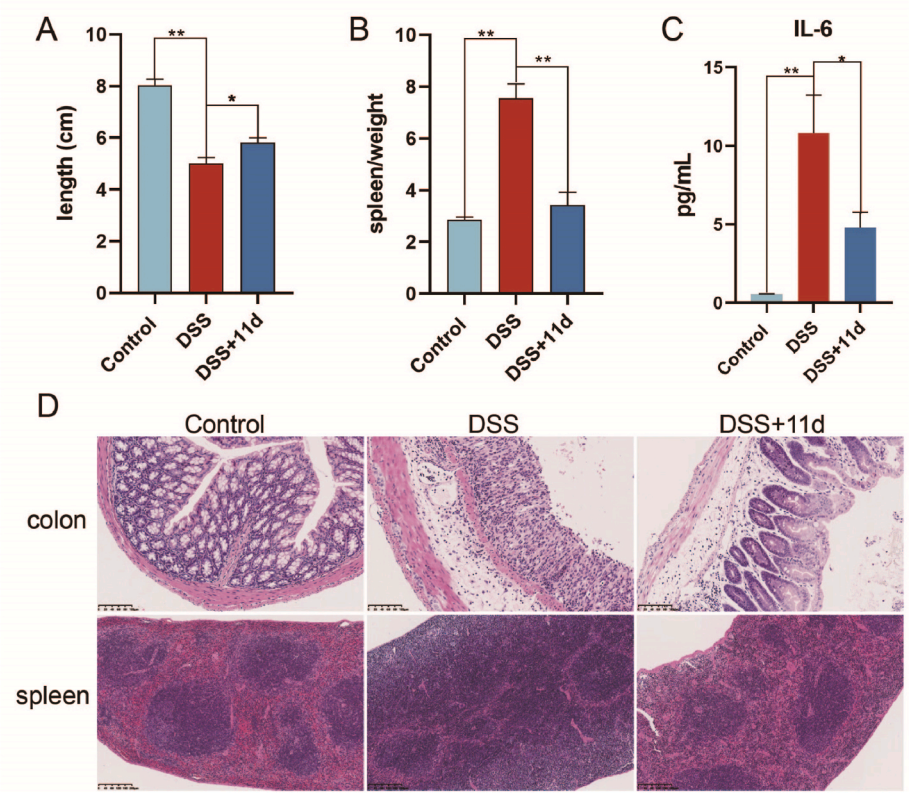

Fig. 8. Effect of **11d** on a mice model of DSS-induced colitis. (A) The length of the colon in each group. (B) The spleen weight of each group was normalized by the weight of the responding mouse. (C) IL-6 level in serum measured by ELISA. (D) H&E staining results of colon tissue (200 ×) and spleen tissue (100 ×). Each bar represents mean ± SEM, n = 5, *, $p < 0.05$, **, $p < 0.01$ vs. the DSS-only group.

Table 5
PK study of **11d** in rats[a].

Perimeters	I.V. (1 mg*kg^{-1})	P.O. (10 mg kg^{-1})
$t_{1/2}$ (h)	1.8 ± 0.4	7.1 ± 7.1
T_{max} (h)	0.14 ± 0.05	2.8 ± 2.8
C_{max} (ng/mL)	1318.7 ± 61.4	167.6 ± 9.2
$AUC_{(0-t)}$ (h*ng/mL)	1112.9 ± 299.6	1057.5 ± 65.1
$AUC_{(0-\infty)}$ (h*ng/mL)	1116.3 ± 297.2	1183.5 ± 276.8
$MRT_{(0-t)}$ (h)	1.1 ± 0.3	7.2 ± 0.6
$MRT_{(0-t)}$ (h)	1.1 ± 0.3	12.3 ± 3.7
Vz (L/kg)	2.3 ± 0.07	0.08 ± 0.06
CL (L/h/kg)	0.9 ± 0.3	0.009 ± 0.002
F (%)	–	10.6 ± 1.0

[a] SD rats weighing 180–220 g were used for the PK study (n = 3). Data were presented by Mean ± SD.

*4.1.5. 2-Chloro-N-(6-methoxypyridin-3-yl)acetamide(**7c**)*

Purple solid in 76.00% yield; mp 118.0–118.8 °C; ^{1}H NMR (400 MHz, Chloroform-*d*) δ 8.23 (d, *J* = 2.7 Hz, 1H), 8.15 (s, 1H), 7.88 (dd, *J* = 8.9, 2.8 Hz, 1H), 6.76 (d, *J* = 8.9 Hz, 1H), 4.21 (s, 2H), 3.93 (s, 3H).

*4.1.6. 2-Chloro-N-(naphthalen-1-yl)acetamide (**7d**)*

White solid in 87.18% yield; mp 163.1–163.7 °C; ^{1}H NMR (400 MHz, DMSO-d_6) δ 10.28 (s, 1H), 8.10–8.02 (m, 1H), 8.01–7.92 (m, 1H), 7.82 (d, *J* = 8.2 Hz, 1H), 7.68 (d, *J* = 7.4 Hz, 1H), 7.65–7.47 (m, 3H), 4.45 (s, 2H).

*4.1.7. N-(naphthalen-1-yl)acrylamide (**7e**)*

Light-yellow solid in 89.02% yield; mp 142.2–142.8 °C; ^{1}H NMR (400 MHz, DMSO-d_6) δ 10.13 (s, 1H), 8.12–8.04 (m, 1H), 8.00–7.91 (m, 1H), 7.79 (dd, *J* = 8.0, 4.9 Hz, 2H), 7.62–7.47 (m, 3H), 6.71 (dd, *J* = 17.0, 10.2 Hz, 1H), 6.32 (dd, *J* = 17.0, 2.0 Hz, 1H), 5.81 (dd, *J* = 10.2, 2.0 Hz, 1H).

*4.1.8. 2-Chloro-N-(pyridin-2-yl)acetamide (**7f**)*

Brown gum in 70.16% yield; ^{1}H NMR (500 MHz, Chloroform-*d*) δ 8.87 (s, 1H), 8.34 (d, *J* = 5.0 Hz, 1H), 8.21 (d, *J* = 8.3 Hz, 1H), 7.75 (t, *J* = 7.9 Hz, 1H), 7.12 (dd, *J* = 7.4, 4.9 Hz, 1H), 4.21 (s, 2H).

*4.1.9. N-(pyridin-2-ylmethyl)ethenesulfonamide (**7g**)*

Brown gum in quantitive yield; ^{1}H NMR (500 MHz, DMSO-d_6) δ 8.49 (d, *J* = 4.9 Hz, 1H), 7.96 (s, 1H), 7.80 (td, *J* = 7.5, 6.9, 3.0 Hz, 1H), 7.45 (dd, *J* = 11.9, 7.8 Hz, 1H), 7.30 (ddd, *J* = 12.7, 7.5, 4.8 Hz, 1H), 6.73 (dd, *J* = 16.5, 10.0 Hz, 1H), 6.03 (d, *J* = 16.5 Hz, 1H), 5.94 (d, *J* = 10.0 Hz, 1H), 4.14 (d, *J* = 4.5 Hz, 2H), 3.24 (t, *J* = 6.8 Hz, 1H).

*4.1.10. N-(6-methoxypyridin-3-yl)ethenesulfonamide (**7h**)*

Black gum in 42.27% yield; ^{1}H NMR (500 MHz, Chloroform-*d*) δ 8.07 (d, *J* = 2.7 Hz, 1H), 7.66 (dd, *J* = 8.9, 2.8 Hz, 1H), 6.79 (d, *J* = 8.7 Hz, 2H), 6.59 (dd, *J* = 16.5, 9.9 Hz, 1H), 6.20 (d, *J* = 16.5 Hz, 1H), 5.98 (d, *J* = 9.9 Hz, 1H), 3.96 (s, 3H).

*4.1.11. N-(naphthalen-1-yl)ethenesulfonamide (**7i**)*

White solid in 73.70% yield; mp 86.5–87.0 °C; ^{1}H NMR (400 MHz, Chloroform-*d*) δ 8.07 (d, *J* = 8.1 Hz, 1H), 7.86 (d, *J* = 7.9 Hz, 1H), 7.75 (d, *J* = 8.2 Hz, 1H), 7.61–7.47 (m, 3H), 7.46–7.40 (m, 1H), 7.27–7.17 (m, 1H), 6.61 (dd, *J* = 16.5, 10.0 Hz, 1H), 6.18 (d, *J* = 16.5 Hz, 1H), 5.83 (d, *J* = 9.8 Hz, 1H).

*4.1.12. N-(quinolin-6-yl)ethenesulfonamide (**7j**)*

Yellow solid in 46.83% yield; ^{1}H NMR (400 MHz, Chloroform-*d*) δ 9.65 (s, 1H), 8.82 (dd, *J* = 4.2, 1.8 Hz, 1H), 8.09 (dd, *J* = 8.3, 1.8 Hz, 1H), 8.01 (dd, *J* = 9.0, 3.2 Hz, 1H), 7.67 (d, *J* = 2.7 Hz, 1H), 7.61 (dt, *J* = 9.1, 2.9 Hz, 1H), 7.38 (dt, *J* = 8.1, 3.7 Hz, 1H), 6.59 (ddd, *J* = 16.5, 9.9,

3.3 Hz, 1H), 6.29 (dd, J = 16.6, 3.2 Hz, 1H), 5.91 (dd, J = 9.9, 3.3 Hz, 1H).

4.1.13. 4-Chloro-3-nitro-N-(pyridin-2-ylmethyl)benzenesulfonamide (7k)

White solid in 90.77% yield; mp 157.1–158.3 °C; ^{1}H NMR (400 MHz, DMSO-d_6) δ 8.71 (s, 1H), 8.37 (dd, J = 5.0, 1.4 Hz, 1H), 8.34 (d, J = 2.1 Hz, 1H), 7.99 (dd, J = 8.5, 2.1 Hz, 1H), 7.93 (d, J = 8.4 Hz, 1H), 7.70 (tt, J = 7.6, 1.2 Hz, 1H), 7.31 (d, J = 7.8 Hz, 1H), 7.21 (dd, J = 7.6, 4.7 Hz, 1H), 4.21 (s, 2H).

4.1.14. General procedure for preparation of intermediates 8a-8f

Excess anhydrous piperazine was dissolved in DCM (20 mL). Various substituted benzyl bromide was added dropwise to the solution at 0 °C. The reaction mixture was stirred for about 2 h at R.T. before water was added. Following extraction with DCM and washing of the organic layer with brine, the DCM layer was dried with anhydrous $MgSO_4$. Products **8b-8e** were obtained through evaporation in vacuo. For the synthesis of **8a**, excess anhydrous piperazine was dissolved in DMSO, then 4-nitro benzene bromide was added and stirred at 80 °C for about 4 h. After completion of the reaction, water was added, followed by extraction with ethyl acetate. The organic layer was washed with brine and dried with anhydrous $MgSO_4$ followed by evaporated in vacuo to obtain desired product **8a**. For the synthesis of **8f**, *N*-Boc piperazine, 2-actamida thiazole, and formaldehyde were dissolved in acetic acid, the mixture was stirred at 100 °C for 1 h and evaporated in vacuo. The crude product was purified by flash silica chromatography (DCM: Methanol = 20 : 1), followed by removal of Boc group with trifluoro acetic acid and evaporation in vacuo to obtain desired compounds.

4.1.15. 1-(4-nitrophenyl)piperazine (8a)

Yellow solid in quantitive yield; mp 120.5–121.4 °C; ^{1}H NMR (400 MHz, Chloroform-*d*) δ 8.17–8.08 (m, 2H), 6.88–6.78 (m, 2H), 3.44 (t, J = 5.1 Hz, 4H), 3.07 (t, J = 5.2 Hz, 4H).

4.1.16. 1-benzylpiperazine (8b)

White solid in 75.76% yield; mp 89.8–90.8 °C; ^{1}H NMR (400 MHz, DMSO-d_6) δ 7.34–7.25 (m, 5H), 3.41 (s, 2H), 2.67 (t, J = 4.9 Hz, 4H), 2.32–2.17 (m, 4H).

4.1.17. 1-(3-nitrobenzyl)piperazine (8c)

Yellow solid in 72.55% yield; mp 106.1–107.5 °C; ^{1}H NMR (400 MHz, DMSO-d_6) δ 8.19–8.07 (m, 2H), 7.77 (d, J = 7.6 Hz, 1H), 7.63 (t, J = 7.8 Hz, 1H), 3.57 (s, 2H), 2.69 (s, 4H), 2.32 (s, 4H).

4.1.18. 1-(4-nitrobenzyl)piperazine (8d)

Yellow solid in 84.92% yield; mp 97.8–99.5 °C; ^{1}H NMR (400 MHz, DMSO-d_6) δ 8.19 (d, J = 8.5 Hz, 2H), 7.59 (d, J = 8.4 Hz, 2H), 3.56 (s, 2H), 2.70 (t, J = 4.8 Hz, 4H), 2.35–2.25 (m, 4H).

4.1.19. 1-(4-methoxybenzyl)piperazine (8e)

White solid in 57.38% yield; mp 104.9–106.3 °C; ^{1}H NMR (400 MHz, Chloroform-*d*) δ 7.25–7.19 (m, 2H), 6.88–6.82 (m, 2H), 3.80 (s, 3H), 3.43 (s, 2H), 2.87 (t, J = 4.9 Hz, 4H), 2.39 (s, 4H), 1.77 (s, 1H).

4.1.20. N-(5-(piperazin-1-ylmethyl)thiazol-2-yl)acetamide(8f)

Yellow solid in 34.10% yield; mp 163.0–164.6 °C; ^{1}H NMR (400 MHz, Chloroform-*d*) δ 11.68 (s, 1H), 7.20 (s, 1H), 3.68 (s, 2H), 3.43 (t, J = 5.0 Hz, 4H), 2.43 (t, J = 5.0 Hz, 4H), 2.31 (s, 3H).

4.1.21. General procedures for preparation of compounds 9a-9z and 10a-10y

To a solution containing intermediate compounds **7a-7j** and triethylamine in DCM at R.T., it was added intermediate **8a-8f**. After the completion of the reaction, the mixture was diluted with water and the aqueous layer was extracted with EtOAc or DCM (3 × 20 mL). The combined organic extracts were dried with anhydrous Na_2SO_4, filtered, and concentrated under reduced pressure. The crude material was purified by chromatography on silica (0–10% methanol in DCM) to obtain the desired compounds.

4.1.22. 2-(4-benzylpiperazin-1-yl)-N-(pyridin-2-ylmethyl)acetamide (9a)

Yellow gum in 75.12% yield; ^{1}H NMR (400 MHz, DMSO-d_6) δ 8.50–8.47 (m, 1H), 8.32 (t, J = 6.0 Hz, 1H), 7.74 (td, J = 7.7, 1.9 Hz, 1H), 7.35–7.21 (m, 8H), 4.40 (d, J = 5.9 Hz, 2H), 3.47 (s, 2H), 2.99 (s, 2H), 2.45 (d, J = 24.2 Hz, 8H). ^{13}C NMR (100 MHz, Chloroform-*d*) δ 170.53, 157.00, 149.12, 137.87, 136.74, 129.13, 128.21, 127.09, 122.29, 121.90, 62.88, 61.50, 53.46, 53.02, 44.09 ppm. MS (ESI, *m/z*): 325.2[M+H]$^+$.

4.1.23. 2-(4-(3-nitrobenzyl)piperazin-1-yl)-N-(pyridin-2-ylmethyl) acetamide (9b)

Brown solid in 30.44% yield; mp 89.8–90.2 °C; ^{1}H NMR (400 MHz, Chloroform-*d*) δ 8.55 (d, J = 7.2 Hz, 1H), 8.20 (s, 1H), 8.16–8.06 (m, 2H), 7.73–7.61 (m, 2H), 7.50 (t, J = 7.9 Hz, 1H), 7.29 (s, 1H), 7.24–7.16 (m, 1H), 4.60 (d, J = 5.6 Hz, 2H), 3.62 (s, 2H), 3.10 (s, 2H), 2.57 (d, J = 30.0 Hz, 8H). ^{13}C NMR (100 MHz, Chloroform-*d*) δ 170.41, 157.01, 149.27, 148.43, 140.57, 136.83, 135.06, 129.29, 123.78, 122.42, 122.37, 122.09, 61.95, 61.53, 53.46, 53.13, 44.19 ppm. MS (ESI, *m/z*): 370.2[M+H]$^+$.

4.1.24. 2-(4-(4-nitrobenzyl)piperazin-1-yl)-N-(pyridin-2-ylmethyl) acetamide (9c)

Yellow solid in 81.09% yield; mp 109.8–111.9 °C; ^{1}H NMR (400 MHz, DMSO-d_6) δ 8.49 (d, J = 4.9 Hz, 1H), 8.34 (t, J = 6.2 Hz, 1H), 8.20 (d, J = 7.6 Hz, 2H), 7.74 (t, J = 7.6 Hz, 1H), 7.60 (d, J = 7.8 Hz, 2H), 7.26 (d, J = 6.9 Hz, 2H), 4.40 (d, J = 5.7 Hz, 2H), 3.62 (s, 2H), 3.00 (s, 2H), 2.33 (s, 8H). ^{13}C NMR (100 MHz, Chloroform-*d*) δ 170.39, 157.01, 149.25, 147.24, 146.22, 136.83, 129.52, 123.61, 122.41, 122.08, 62.03, 61.55, 53.49, 53.22, 44.18 ppm. MS (ESI, *m/z*): 370.2[M+H]$^+$.

4.1.25. 2-(4-(4-nitrophenyl)piperazin-1-yl)-N-(pyridin-2-ylmethyl) acetamide (9d)

Yellow solid in 7.27% yield; mp 135.6–136.9 °C; ^{1}H NMR (400 MHz, Chloroform-*d*) δ 8.55 (d, J = 4.9 Hz, 1H), 8.18 (d, J = 6.0 Hz, 1H), 8.16–8.11 (m, 2H), 7.68 (t, J = 7.7 Hz, 1H), 7.29 (s, 1H), 7.21 (dd, J = 7.5, 4.9 Hz, 1H), 6.87–6.80 (m, 2H), 4.62 (d, J = 5.3 Hz, 2H), 3.53–3.43 (m, 4H), 3.18 (s, 2H), 2.78–2.67 (m, 4H). ^{13}C NMR (100 MHz, Chloroform-*d*) δ 169.79, 156.53, 154.82, 149.19, 138.80, 136.96, 126.00, 122.55, 122.23, 112.94, 61.52, 53.01, 47.22, 44.02 ppm. MS (ESI, *m/z*): 356.2[M+H]$^+$.

4.1.26. N-(pyridin-2-ylmethyl)-2-(4-(pyrimidin-2-yl)piperazin-1-yl) acetamide (9e)

White solid in 69.98% yield; mp 111.2–112.9 °C; ^{1}H NMR (400 MHz, Chloroform-*d*) δ 8.56 (dd, J = 5.1, 1.8 Hz, 1H), 8.31 (d, J = 4.7 Hz, 2H), 8.23 (s, 1H), 7.67 (td, J = 7.7, 1.8 Hz, 1H), 7.28 (d, J = 7.6 Hz, 1H), 7.20 (dd, J = 7.6, 4.9 Hz, 1H), 6.50 (t, J = 4.7 Hz, 1H), 4.63 (d, J = 5.4 Hz, 2H), 3.93–3.83 (m, 4H), 3.14 (s, 2H), 2.65–2.57 (m, 4H). ^{13}C NMR (100 MHz, Chloroform-*d*) δ 170.25, 161.64, 157.77, 156.83, 149.28, 136.79, 122.41, 122.03, 110.09, 61.75, 53.40, 44.09, 43.78 ppm. MS (ESI, *m/z*): 313.2[M+H]$^+$.

4.1.27. 2-(4-(4-methoxybenzyl)piperazin-1-yl)-N-(pyridin-2-ylmethyl) acetamide (9f)

Yellow gum in 62.02% yield; ^{1}H NMR (400 MHz, DMSO-d_6) δ 8.48 (dd, J = 5.3, 1.9 Hz, 1H), 8.32 (t, J = 6.0 Hz, 1H), 7.74 (td, J = 7.7, 1.8 Hz, 1H), 7.29–7.15 (m, 4H), 6.92–6.83 (m, 2H), 4.39 (d, J = 5.9 Hz, 2H), 3.73 (s, 3H), 3.40 (s, 3H), 2.98 (s, 2H), 2.43 (d, J = 29.3 Hz, 8H). ^{13}C NMR (100 MHz, Chloroform-*d*) δ 170.67, 158.83, 157.09, 149.24, 136.85, 130.44, 129.85, 122.40, 122.04, 113.67, 62.32, 61.55, 55.30, 53.52, 52.98, 44.19 ppm. MS (ESI, *m/z*): 355.2[M+H]$^+$.

*4.1.28. 2-(4-((2-acetamidothiazol-5-yl)methyl)piperazin-1-yl)-N-(pyridin-2-ylmethyl)acetamide (**9g**)*

Yellow solid in 16.54% yield; mp 159.0–160.7 °C; ^{1}H NMR (400 MHz, DMSO-d_6) δ 11.96 (s, 1H), 8.50–8.46 (m, 1H), 8.34 (t, J = 6.0 Hz, 1H), 7.75 (td, J = 7.7, 1.8 Hz, 1H), 7.26 (d, J = 7.5 Hz, 3H), 4.40 (d, J = 5.9 Hz, 2H), 3.65 (s, 2H), 3.01 (s, 2H), 2.48 (s, 8H), 2.12 (s, 3H). ^{13}C NMR (100 MHz, Chloroform-*d*) δ 170.48, 168.10, 160.09, 157.03, 149.24, 136.87, 134.52, 129.30, 122.43, 122.11, 61.44, 54.15, 53.37, 52.68, 45.87, 44.18 ppm. MS (ESI, *m/z*): 389.2[M+H]$^+$.

*4.1.29. 3-(4-benzylpiperazin-1-yl)-N-(pyridin-2-ylmethyl)propanamide (**9h**)*

Yellow gum in 44.66% yield; ^{1}H NMR (400 MHz, DMSO-d_6) δ 8.68 (t, J = 5.9 Hz, 1H), 8.48 (d, J = 4.6 Hz, 1H), 7.72 (t, J = 7.6 Hz, 1H), 7.38–7.30 (m, 5H), 7.26 (dd, J = 7.5, 4.9 Hz, 1H), 4.36 (d, J = 5.8 Hz, 2H), 3.69 (s, 2H), 3.01–2.77 (m, 8H), 2.68 (s, 2H), 2.55 (s, 2H). ^{13}C NMR (100 MHz, Chloroform-*d*) δ 171.09, 156.88, 149.05, 136.89, 135.93, 129.57, 128.62, 127.91, 122.41, 122.11, 62.20, 53.36, 51.98, 51.13, 44.71, 31.71 ppm. MS (ESI, *m/z*): 339.2[M+H]$^+$.

*4.1.30. 3-(4-(4-nitrobenzyl)piperazin-1-yl)-N-(pyridin-2-ylmethyl) propanamide (**9i**)*

Yellow gum in 31.07% yield; ^{1}H NMR (400 MHz, DMSO-d_6) δ 8.61 (t, J = 5.9 Hz, 1H), 8.48 (ddd, J = 4.8, 1.8, 0.9 Hz, 1H), 8.24–8.18 (m, 2H), 7.71 (td, J = 7.7, 1.8 Hz, 1H), 7.63–7.57 (m, 2H), 7.37 (dt, J = 7.8, 1.1 Hz, 1H), 7.25 (ddd, J = 7.5, 4.8, 1.2 Hz, 1H), 4.35 (d, J = 5.9 Hz, 2H), 3.61 (s, 2H), 2.56 (t, J = 6.9 Hz, 2H), 2.41 (s, 8H), 2.34 (t, J = 6.9 Hz, 2H). ^{13}C NMR (100 MHz, Chloroform-*d*) δ 172.50, 157.17, 149.05, 147.26, 146.17, 136.80, 129.54, 123.63, 122.32, 122.07, 62.12, 53.81, 52.96, 52.52, 44.72, 32.37 ppm. MS (ESI, *m/z*): 384.2[M+H]$^+$.

*4.1.31. 3-(4-(4-nitrophenyl)piperazin-1-yl)-N-(pyridin-2-ylmethyl) propanamide (**9j**)*

Yellow solid in 30.86% yield; mp 143.4–144.1 °C; ^{1}H NMR (400 MHz, DMSO-d_6) δ 8.60 (t, J = 5.9 Hz, 1H), 8.48 (dt, J = 4.6, 1.5 Hz, 1H), 8.11–8.01 (m, 2H), 7.73 (td, J = 7.7, 1.8 Hz, 1H), 7.36 (d, J = 7.9 Hz, 1H), 7.24 (ddd, J = 7.7, 4.8, 1.1 Hz, 1H), 7.09–7.01 (m, 2H), 4.37 (d, J = 5.9 Hz, 2H), 3.46 (d, J = 5.0 Hz, 4H), 2.63 (t, J = 6.9 Hz, 2H), 2.54 (d, J = 5.1 Hz, 4H), 2.39 (t, J = 6.9 Hz, 2H). ^{13}C NMR (100 MHz, Chloroform-*d*) δ 172.05, 156.67, 154.84, 148.95, 138.72, 136.78, 126.03, 122.43, 122.14, 112.86, 53.79, 52.12, 46.97, 44.65, 32.54 ppm. MS (ESI, *m/z*): 370.2[M+H]$^+$.

*4.1.32. 2-(4-benzylpiperazin-1-yl)-N-(6-methoxypyridin-3-yl)acetamide (**9k**)*

Pink solid in 46.50% yield; mp 92.2–93.4 °C; ^{1}H NMR (400 MHz, Chloroform-*d*) δ 9.05 (s, 1H), 8.22 (d, J = 2.7 Hz, 1H), 7.95 (dd, J = 8.8, 2.8 Hz, 1H), 7.36–7.22 (m, 5H), 6.73 (d, J = 8.8 Hz, 1H), 3.91 (s, 3H), 3.54 (s, 2H), 3.13 (s, 2H), 2.64 (t, J = 4.8 Hz, 5H), 2.53 (s, 4H). ^{13}C NMR (100 MHz, Chloroform-*d*) δ 168.79, 161.01, 138.18, 137.76, 131.72, 129.23, 128.44, 128.37, 127.30, 110.66, 62.94, 61.76, 53.62, 53.57, 53.16 ppm. MS (ESI, *m/z*): 341.2[M+H]$^+$.

*4.1.33. N-(6-methoxypyridin-3-yl)-2-(4-(3-nitrobenzyl)piperazin-1-yl) acetamide (**9l**)*

Orange gum in 96.30% yield; ^{1}H NMR (400 MHz, Chloroform-*d*) δ 9.02 (s, 1H), 8.25–8.19 (m, 2H), 8.15–8.10 (m, 1H), 7.95 (dd, J = 8.9, 2.8 Hz, 1H), 7.69 (d, J = 7.6 Hz, 1H), 7.51 (t, J = 7.9 Hz, 1H), 6.74 (d, J = 8.8 Hz, 1H), 3.91 (s, 3H), 3.64 (s, 2H), 3.17 (s, 2H), 2.69 (d, J = 4.9 Hz, 4H), 2.57 (s, 4H). ^{13}C NMR (100 MHz, Chloroform-*d*) δ 168.55, 148.37, 140.41, 138.14, 134.95, 131.64, 129.27, 128.33, 123.63, 122.32, 110.57, 61.82, 61.67, 53.55, 53.45, 53.11 ppm. MS (ESI, *m/z*): 386.2 [M+H]$^+$.

*4.1.34. N-(6-methoxypyridin-3-yl)-2-(4-(4-nitrobenzyl)piperazin-1-yl) acetamide (**9m**)*

Brown solid in 80.68% yield; mp 111.3–112.6 °C; ^{1}H NMR (400 MHz, Chloroform-*d*) δ 9.00 (s, 1H), 8.24–8.15 (m, 3H), 7.96 (dd, J = 8.9, 2.7 Hz, 1H), 7.52 (d, J = 8.5 Hz, 2H), 6.74 (d, J = 8.8 Hz, 1H), 3.91 (s, 3H), 3.64 (s, 2H), 3.16 (s, 2H), 2.75–2.63 (m, 4H), 2.56 (s, 4H). MS (ESI, *m/z*): 386.2[M+H]$^+$.

*4.1.35. N-(6-methoxypyridin-3-yl)-2-(4-(4-nitrophenyl)piperazin-1-yl) acetamide (**9n**)*

Yellow solid in 72.65% yield; mp 233.8–234.7 °C; ^{1}H NMR (400 MHz, DMSO-d_6) δ 9.83 (s, 1H), 8.39 (d, J = 2.6 Hz, 1H), 8.10–8.01 (m, 2H), 7.94 (dd, J = 8.9, 2.7 Hz, 1H), 7.09–6.99 (m, 2H), 6.80 (d, J = 8.9 Hz, 1H), 3.82 (s, 3H), 3.54 (t, J = 5.1 Hz, 4H), 3.21 (s, 2H), 2.66 (t, J = 5.1 Hz, 4H). ^{13}C NMR (100 MHz, DMSO-d_6) δ 168.74, 160.29, 155.24, 138.78, 137.38, 132.56, 130.03, 126.27, 113.18, 110.48, 61.67, 53.67, 52.73, 46.75 ppm. MS (ESI, *m/z*): 372.2[M+H]$^+$.

*4.1.36. N-(6-methoxypyridin-3-yl)-2-(4-(pyrimidin-2-yl)piperazin-1-yl) acetamide (**9o**)*

White solid in 82.60% yield; mp 164.5–164.9 °C; ^{1}H NMR (500 MHz, Chloroform-*d*) δ 9.04 (s, 1H), 8.33 (d, J = 4.8 Hz, 2H), 8.24 (d, J = 2.7 Hz, 1H), 7.99 (dd, J = 8.9, 2.8 Hz, 1H), 6.76 (d, J = 8.9 Hz, 1H), 6.54 (t, J = 4.8 Hz, 1H), 3.92 (d, J = 4.4 Hz, 7H), 3.21 (s, 2H), 2.70 (t, J = 5.1 Hz, 4H). ^{13}C NMR (100 MHz, Chloroform-*d*) δ 168.34, 161.58, 161.08, 157.81, 138.23, 131.74, 128.34, 110.70, 110.37, 62.00, 53.62, 53.46, 43.79 ppm. MS (ESI, *m/z*): 329.2[M+H]$^+$.

*4.1.37. 2-(4-(4-methoxybenzyl)piperazin-1-yl)-N-(6-methoxypyridin-3-yl)acetamide (**9p**)*

White solid in 85.57% yield; mp 126.9–127.7 °C; ^{1}H NMR (400 MHz, Chloroform-*d*) δ 9.03 (s, 1H), 8.20 (d, J = 2.7 Hz, 1H), 7.96 (dd, J = 8.8, 2.8 Hz, 1H), 7.23 (d, J = 8.4 Hz, 3H), 6.91–6.83 (m, 2H), 6.74 (d, J = 8.8 Hz, 1H), 3.92 (s, 3H), 3.81 (s, 3H), 3.49 (s, 2H), 3.14 (s, 2H), 2.71–2.42 (m, 8H). ^{13}C NMR (100 MHz, Chloroform-*d*) δ 168.75, 161.03, 158.91, 138.14, 131.67, 130.41, 129.77, 128.45, 113.73, 110.68, 62.32, 61.77, 55.33, 53.62, 53.08 ppm. MS (ESI, *m/z*): 371.3[M+H]$^+$.

*4.1.38. 2-(4-((2-acetamidothiazol-5-yl)methyl)piperazin-1-yl)-N-(6-methoxypyridin-3-yl)acetamide (**9q**)*

Pink solid in 19.05% yield; mp 180.6–182.6 °C; ^{1}H NMR (400 MHz, DMSO-d_6) δ 11.97 (s, 1H), 9.74 (s, 1H), 8.37 (d, J = 2.7 Hz, 1H), 7.91 (dd, J = 8.9, 2.7 Hz, 1H), 7.28 (s, 1H), 6.79 (d, J = 8.9 Hz, 1H), 3.81 (s, 3H), 3.67 (s, 2H), 3.14 (s, 2H), 2.54 (s, 8H), 2.12 (s, 3H). ^{13}C NMR (100 MHz, Chloroform-*d*) δ 168.43, 168.10, 161.07, 160.20, 138.17, 134.63, 131.73, 128.37, 110.69, 61.57, 54.09, 53.65, 53.36, 52.64, 23.23 ppm. MS (ESI, *m/z*): 405.2[M+H]$^+$.

*4.1.39. 2-(4-benzylpiperazin-1-yl)-N-(naphthalen-1-yl)acetamide (**9r**)*

Light-yellow solid in 98.18% yield; mp 89.9–90.6 °C; ^{1}H NMR (400 MHz, Chloroform-*d*) δ 9.95 (s, 1H), 8.25 (dd, J = 7.6, 1.1 Hz, 1H), 7.85 (ddd, J = 13.3, 8.0, 1.6 Hz, 2H), 7.65 (d, J = 8.2 Hz, 1H), 7.58–7.45 (m, 3H), 7.37–7.31 (m, 4H), 7.30–7.23 (m, 1H), 3.59 (s, 2H), 3.27 (s, 2H), 2.86–2.52 (m, 8H). ^{13}C NMR (100 MHz, Chloroform-*d*) δ 168.60, 134.14, 132.33, 129.29, 129.06, 128.43, 127.39, 126.31, 126.14, 125.95, 124.84, 119.92, 118.29, 62.94, 62.29, 53.63, 53.43 ppm. MS (ESI, *m/z*): 360.2[M+H]$^+$.

*4.1.40. N-(naphthalen-1-yl)-2-(4-(3-nitrobenzyl)piperazin-1-yl)acetamide (**9s**)*

Yellow gum in 71.11% yield; ^{1}H NMR (400 MHz, DMSO-d_6) δ 9.99 (s, 1H), 8.19 (t, J = 2.0 Hz, 1H), 8.14 (ddd, J = 8.2, 2.5, 1.1 Hz, 1H), 7.99–7.90 (m, 2H), 7.87 (dd, J = 7.5, 1.1 Hz, 1H), 7.83–7.73 (m, 2H), 7.65 (t, J = 7.9 Hz, 1H), 7.61–7.53 (m, 2H), 7.50 (dd, J = 8.2, 7.5 Hz, 1H), 3.68 (s, 2H), 3.28 (s, 2H), 2.62 (d, J = 46.4 Hz, 8H). ^{13}C NMR (100 MHz, Chloroform-*d*) δ 168.54, 148.45, 140.55, 135.06, 134.14, 132.33,

129.38, 129.07, 126.37, 126.10, 126.01, 124.91, 123.71, 122.41, 119.92, 118.40, 62.27, 61.90, 53.62, 53.47 ppm. MS (ESI, *m/z*): 405.2 $[M+H]^+$.

4.1.41. N-(naphthalen-1-yl)-2-(4-(4-nitrobenzyl)piperazin-1-yl)acetamide (9t)

Yellow solid in 68.94% yield; mp 189.1–190.9 °C; ^{1}H NMR (400 MHz, DMSO-d_6) δ 9.99 (s, 1H), 8.26–8.16 (m, 2H), 8.00–7.89 (m, 2H), 7.86 (d, J = 7.4 Hz, 1H), 7.77 (d, J = 8.2 Hz, 1H), 7.63 (d, J = 6.9 Hz, 1H), 7.62–7.55 (m, 3H), 7.52 (q, J = 7.6 Hz, 1H), 3.68 (s, 2H), 3.29 (s, 2H), 2.69 (s, 4H), 2.56 (s, 4H). ^{13}C NMR (100 MHz, Chloroform-*d*) δ 168.41, 147.37, 146.00, 134.15, 132.24, 129.54, 129.11, 126.31, 126.14, 125.97, 124.96, 123.72, 119.85, 118.46, 62.26, 62.03, 53.62, 53.55 ppm. MS (ESI, *m/z*): 405.2$[M+H]^+$.

4.1.42. N-(naphthalen-1-yl)-2-(4-(4-nitrophenyl)piperazin-1-yl)acetamide (9u)

Yellow solid in 48.68% yield; mp 216.4–218.0 °C; ^{1}H NMR (400 MHz, DMSO-d_6) δ 10.02 (s, 1H), 8.11–8.05 (m, 2H), 7.97 (ddd, J = 7.3, 3.3, 1.4 Hz, 2H), 7.80 (dd, J = 13.3, 7.8 Hz, 2H), 7.64–7.47 (m, 3H), 7.12–7.03 (m, 2H), 3.61 (t, J = 5.0 Hz, 4H), 2.78 (t, J = 5.1 Hz, 4H). ^{13}C NMR (100 MHz, Chloroform-*d*) δ 167.77, 154.66, 139.19, 134.15, 132.02, 129.19, 126.48, 126.11, 126.06, 126.01, 125.20, 119.61, 118.64, 113.24, 62.34, 53.21, 47.53 ppm. MS (ESI, *m/z*): 391.2$[M+H]^+$.

4.1.43. N-(naphthalen-1-yl)-2-(4-(pyrimidin-2-yl)piperazin-1-yl) acetamide (9v)

White solid in 86.16% yield; mp 195.0–196.3 °C; ^{1}H NMR (400 MHz, Chloroform-*d*) δ 9.95 (s, 1H), 8.35 (d, J = 4.8 Hz, 2H), 8.28 (dd, J = 7.6, 1.2 Hz, 1H), 7.87 (ddd, J = 9.4, 7.7, 1.5 Hz, 2H), 7.71–7.65 (m, 1H), 7.59–7.48 (m, 3H), 6.55 (t, J = 4.8 Hz, 1H), 4.06–3.96 (m, 4H), 3.35 (s, 2H), 2.81 (t, J = 5.1 Hz, 4H). ^{13}C NMR (100 MHz, Chloroform-*d*) δ 168.24, 161.68, 157.88, 134.14, 132.21, 129.10, 126.46, 126.12, 126.02, 125.93, 124.98, 119.74, 118.40, 110.50, 62.55, 53.59, 44.08 ppm. MS (ESI, *m/z*): 348.2$[M+H]^+$.

4.1.44. 2-(4-(4-methoxybenzyl)piperazin-1-yl)-N-(naphthalen-1-yl) acetamide (9w)

Brown solid in 74.37% yield; mp 99.0–100.9 °C; ^{1}H NMR (400 MHz, Chloroform-*d*) δ 9.96 (s, 1H), 8.25 (dd, J = 7.6, 1.1 Hz, 1H), 7.91–7.80 (m, 2H), 7.65 (d, J = 8.2 Hz, 1H), 7.59–7.44 (m, 3H), 7.29–7.22 (m, 2H), 6.92–6.84 (m, 2H), 3.80 (s, 3H), 3.53 (s, 2H), 3.27 (s, 2H), 2.79–2.52 (m, 8H). ^{13}C NMR (100 MHz, Chloroform-*d*) δ 168.64, 158.94, 132.35, 130.43, 129.77, 129.06, 126.30, 126.14, 125.94, 124.81, 119.93, 118.24, 113.75, 62.35, 62.30, 55.34, 53.69, 53.35 ppm. MS (ESI, *m/z*): 390.2$[M+H]^+$.

4.1.45. 3-(4-benzylpiperazin-1-yl)-N-(naphthalen-1-yl)propanamide (9x)

White solid in 23.73% yield; mp 203.5–205.4 °C; ^{1}H NMR (400 MHz, DMSO-d_6) δ 10.28 (s, 1H), 8.13 (d, J = 8.4 Hz, 1H), 7.94 (dd, J = 8.2, 1.3 Hz, 1H), 7.76 (t, J = 8.0 Hz, 2H), 7.55 (ddd, J = 8.1, 6.8, 1.2 Hz, 1H), 7.51–7.43 (m, 2H), 7.38–7.22 (m, 5H), 3.50 (s, 2H), 2.71 (t, J = 6.6 Hz, 2H), 2.61 (t, J = 6.5 Hz, 4H), 2.54 (s, 2H), 2.47 (s, 4H). ^{13}C NMR (100 MHz, Chloroform-*d*) δ 171.04, 137.69, 134.11, 133.70, 129.30, 128.85, 128.45, 127.35, 126.23, 126.10, 125.82, 125.75, 124.33, 121.47, 118.76, 63.10, 54.42, 52.95, 52.69, 32.95 ppm. MS (ESI, *m/z*): 374.3 $[M+H]^+$.

4.1.46. N-(naphthalen-1-yl)-3-(4-(4-nitrophenyl)piperazin-1-yl) propanamide (9y)

Yellow solid in 87.00% yield; mp 193.8–195.2 °C; ^{1}H NMR (400 MHz, DMSO-d_6) δ 10.12 (s, 1H), 8.17–8.11 (m, 1H), 8.09–8.05 (m, 2H), 7.96–7.91 (m, 1H), 7.74 (dd, J = 15.2, 7.9 Hz, 3H), 7.55–7.46 (m, 3H), 7.07 (d, J = 9.5 Hz, 2H), 3.52 (t, J = 4.9 Hz, 4H), 2.78 (t, J = 6.7 Hz, 2H), 2.67 (dt, J = 10.1, 5.8 Hz, 8H). ^{13}C NMR (100 MHz, DMSO-d_6) δ 171.26, 155.26, 137.45, 134.24, 134.20, 128.65, 128.11, 126.50, 126.22, 125.56, 123.30, 121.77, 113.20, 113.02, 54.43, 52.60, 46.90, 34.17 ppm. MS (ESI, *m/z*): 405.2$[M+H]^+$.

4.1.47. 2-(4-(4-nitrophenyl)piperazin-1-yl)-N-(pyridin-2-yl)acetamide (9z)

Yellow solid in 55.42% yield; mp 167.4–169.4 °C; ^{1}H NMR (500 MHz, DMSO-d_6) δ 10.04 (s, 1H), 8.31 (d, J = 4.8 Hz, 1H), 8.10 (d, J = 8.3 Hz, 1H), 8.05 (d, J = 9.1 Hz, 2H), 7.80 (t, J = 7.7 Hz, 1H), 7.12 (dd, J = 7.3, 4.9 Hz, 1H), 7.04 (d, J = 9.1 Hz, 2H), 3.52 (t, J = 5.0 Hz, 4H), 3.28 (s, 2H), 2.68 (t, J = 5.0 Hz, 4H). ^{13}C NMR (100 MHz, Chloroform-*d*) δ 168.46, 154.74, 150.84, 147.98, 138.99, 138.60, 126.00, 120.16, 114.00, 113.12, 62.15, 53.05, 47.24 ppm. MS (ESI, *m/z*): 342.2$[M+H]^+$.

4.1.48. 2-(4-benzylpiperazin-1-yl)-N-(pyridin-2-ylmethyl)ethane-1-sulfonamide (10a)

Brown gum in 72.20% yield; ^{1}H NMR (500 MHz, Chloroform-*d*) δ 8.55 (d, J = 4.9 Hz, 1H), 7.72 (t, J = 7.6 Hz, 1H), 7.37 (d, J = 7.9 Hz, 1H), 7.35–7.27 (m, 5H), 7.27–7.24 (m, 1H), 4.43 (s, 2H), 3.49 (s, 2H), 3.20 (t, J = 6.6 Hz, 2H), 2.88 (t, J = 6.6 Hz, 2H), 2.09 (s, 2H). ^{13}C NMR (100 MHz, Chloroform-*d*) δ 156.07, 149.03, 137.11, 137.03, 129.36, 128.29, 127.33, 122.82, 122.21, 62.62, 52.62, 52.48, 52.39, 49.06, 47.62, 25.33 ppm. MS (ESI, *m/z*): 375.2$[M+H]^+$.

4.1.49. 2-(4-(3-nitrobenzyl)piperazin-1-yl)-N-(pyridin-2-ylmethyl)ethane-1-sulfonamide (10b)

Brown solid in 28.01% yield; mp 91.9–93.3 °C; ^{1}H NMR (500 MHz, Chloroform-*d*) δ 8.55 (d, J = 4.9 Hz, 1H), 7.72 (t, J = 7.6 Hz, 1H), 7.37 (d, J = 7.9 Hz, 1H), 7.35–7.27 (m, 5H), 7.27–7.24 (m, 1H), 4.43 (s, 2H), 3.49 (s, 2H), 3.20 (t, J = 6.6 Hz, 2H), 2.88 (t, J = 6.6 Hz, 2H), 2.51 (s, 8H). ^{13}C NMR (100 MHz, Chloroform-*d*) δ 156.05, 149.21, 148.42, 140.50, 137.07, 135.06, 129.29, 123.73, 122.88, 122.36, 122.19, 61.88, 52.97, 52.84, 52.60, 49.08, 47.75 ppm. MS (ESI, *m/z*): 420.2$[M+H]^+$.

4.1.50. 2-(4-(4-nitrobenzyl)piperazin-1-yl)-N-(pyridin-2-ylmethyl)ethane-1-sulfonamide (10c)

Brown solid in 38.27% yield; mp 119.6–120.7 °C; ^{1}H NMR (400 MHz, Chloroform-*d*) δ 8.54 (d, J = 4.4 Hz, 1H), 8.16 (d, J = 8.5 Hz, 2H), 7.71 (t, J = 7.7 Hz, 1H), 7.48 (d, J = 8.5 Hz, 2H), 7.36 (d, J = 7.8 Hz, 1H), 7.25 (dd, J = 7.6, 4.9 Hz, 1H), 6.20 (s, 1H), 4.43 (s, 2H), 3.55 (s, 2H), 3.20 (t, J = 6.6 Hz, 2H), 2.88 (t, J = 6.6 Hz, 2H), 2.48 (d, J = 30.1 Hz, 8H). ^{13}C NMR (100 MHz, Chloroform-*d*) δ 156.03, 149.19, 147.25, 146.10, 137.06, 129.52, 123.61, 122.86, 122.18, 62.00, 53.02, 52.95, 52.62, 49.11, 47.73 ppm. MS (ESI, *m/z*): 420.2$[M+H]^+$.

4.1.51. 2-(4-(4-nitrophenyl)piperazin-1-yl)-N-(pyridin-2-ylmethyl)ethane-1-sulfonamide (10d)

Yellow solid in 45.96% yield; mp 186.4–187.3 °C; ^{1}H NMR (500 MHz, DMSO-d_6) δ 8.50 (d, J = 5.4 Hz, 1H), 8.04 (t, J = 6.7 Hz, 2H), 7.80 (q, J = 6.7 Hz, 1H), 7.68 (q, J = 5.9 Hz, 1H), 7.45 (t, J = 6.0 Hz, 1H), 7.29 (d, J = 6.5 Hz, 1H), 7.03 (t, J = 6.8 Hz, 2H), 4.28 (t, J = 5.6 Hz, 2H), 3.56–3.39 (m, 7H), 3.28 (q, J = 6.8 Hz, 3H), 2.70 (d, J = 7.1 Hz, 2H). ^{13}C NMR (100 MHz, Chloroform-*d*) δ 155.52, 154.76, 149.14, 138.81, 137.14, 126.00, 123.00, 122.24, 112.91, 52.68, 52.61, 49.22, 47.47, 46.92 ppm. MS (ESI, *m/z*): 406.2$[M+H]^+$.

4.1.52. N-(pyridin-2-ylmethyl)-2-(4-(pyrimidin-2-yl)piperazin-1-yl) ethane-1-sulfonamide (10e)

White solid in 12.50% yield; mp 98.9–100.0 °C; ^{1}H NMR (500 MHz, Chloroform-*d*) δ 8.52 (d, J = 4.9 Hz, 1H), 8.30 (d, J = 4.8 Hz, 2H), 7.69 (t, J = 7.7 Hz, 1H), 7.33 (d, J = 7.8 Hz, 1H), 7.22 (dd, J = 7.5, 4.9 Hz, 1H), 6.50 (t, J = 4.7 Hz, 1H), 6.22 (t, J = 5.7 Hz, 1H), 4.46 (d, J = 5.2 Hz, 2H), 3.81 (t, J = 5.0 Hz, 4H), 3.25 (t, J = 6.5 Hz, 2H), 2.91 (t, J = 6.5 Hz, 2H), 2.53 (t, J = 5.0 Hz, 4H). ^{13}C NMR (100 MHz, Chloroform-*d*) δ 161.57, 157.81, 155.71, 149.27, 137.03, 122.90, 122.10, 110.16, 53.04, 52.90, 49.18, 47.56, 43.44 ppm. MS (ESI, *m/z*): 363.2$[M+H]^+$.

*4.1.53. 2-(4-(4-methoxybenzyl)piperazin-1-yl)-N-(pyridin-2-ylmethyl) ethane-1-sulfonamide (**10f**)*

Yellow gum in 45.57% yield; ^{1}H NMR (400 MHz, DMSO-d_6) δ 8.51 (dd, J = 5.0, 1.7 Hz, 1H), 7.81 (td, J = 7.7, 1.8 Hz, 1H), 7.62 (t, J = 6.3 Hz, 1H), 7.44 (d, J = 7.8 Hz, 1H), 7.30 (dd, J = 7.4, 4.9 Hz, 1H), 7.21–7.14 (m, 2H), 6.90–6.83 (m, 2H), 4.26 (d, J = 5.9 Hz, 2H), 3.73 (s, 3H), 3.25–3.14 (m, 2H), 2.62 (dd, J = 8.5, 6.3 Hz, 2H), 2.34 (d, J = 19.4 Hz, 7H). ^{13}C NMR (100 MHz, Chloroform-*d*) δ 158.89, 156.09, 149.23, 137.04, 130.48, 129.62, 122.83, 122.16, 113.70, 62.30, 55.32, 52.99, 52.73, 52.65, 49.01, 47.73 ppm. MS (ESI, *m/z*): 405.2[M+H]$^+$.

*4.1.54. 2-(4-benzylpiperazin-1-yl)-N-(6-methoxypyridin-3-yl)ethane-1-sulfonamide (**10g**)*

Yellow gum in 26.43% yield; ^{1}H NMR (400 MHz, DMSO-d_6) δ 10.20–9.14 (brs, 1H), 8.03 (d, J = 2.7 Hz, 1H), 7.58 (dd, J = 8.9, 2.8 Hz, 1H), 7.34–7.20 (m, 5H), 6.82 (d, J = 8.8 Hz, 1H), 3.83 (s, 3H), 3.42 (s, 2H), 3.19 (dd, J = 8.7, 6.1 Hz, 2H), 2.69 (dd, J = 8.7, 6.1 Hz, 2H), 2.33 (d, J = 19.8 Hz, 8H). ^{13}C NMR (100 MHz, Chloroform-*d*) δ 162.32, 141.05, 137.68, 135.24, 129.11, 128.30, 127.23, 127.00, 111.42, 62.83, 53.72, 53.15, 53.02, 52.68, 48.32 ppm. MS (ESI, *m/z*): 391.2[M+H]$^+$.

*4.1.55. N-(6-methoxypyridin-3-yl)-2-(4-(3-nitrobenzyl)piperazin-1-yl) ethane-1-sulfonamide (**10h**)*

Brown gum in 90.96% yield; ^{1}H NMR (400 MHz, DMSO-d_6) δ 8.13 (s, 2H), 8.02 (d, J = 2.8 Hz, 1H), 7.75 (d, J = 7.6 Hz, 1H), 7.65–7.60 (m, 1H), 7.57 (dd, J = 8.8, 2.8 Hz, 1H), 6.82 (d, J = 8.8 Hz, 1H), 3.82 (s, 3H), 3.58 (s, 2H), 3.23–3.16 (m, 2H), 2.73–2.65 (m, 2H), 2.36 (s, 8H). ^{13}C NMR (100 MHz, Chloroform-*d*) δ 162.29, 148.36, 141.18, 140.37, 135.12, 134.99, 129.25, 127.02, 123.63, 122.31, 111.34, 61.72, 53.73, 52.96, 52.89, 52.36, 48.40 ppm. MS (ESI, *m/z*): 436.2[M+H]$^+$.

*4.1.56. N-(6-methoxypyridin-3-yl)-2-(4-(4-nitrobenzyl)piperazin-1-yl) ethane-1-sulfonamide (**10i**)*

Brown solid in 9.31% yield; mp 88.9–90.0 °C; ^{1}H NMR (400 MHz, DMSO-d_6) δ 8.23–8.15 (m, 2H), 8.02 (d, J = 2.7 Hz, 1H), 7.62–7.53 (m, 3H), 6.82 (d, J = 8.8 Hz, 1H), 3.82 (s, 3H), 3.57 (s, 2H), 3.20 (dd, J = 8.5, 6.2 Hz, 2H), 2.69 (dd, J = 8.6, 6.1 Hz, 2H), 2.36 (s, 8H). ^{13}C NMR (100 MHz, Chloroform-*d*) δ 162.51, 147.39, 141.19, 135.43, 129.57, 126.98, 123.72, 111.59, 61.84, 53.80, 53.08, 52.96, 52.61, 48.24 ppm. MS (ESI, *m/z*): 436.1[M+H]$^+$.

*4.1.57. N-(6-methoxypyridin-3-yl)-2-(4-(4-nitrophenyl)piperazin-1-yl) ethane-1-sulfonamide (**10j**)*

Yellow gum in 14.49% yield; ^{1}H NMR (500 MHz, Chloroform-*d*) δ 8.09 (d, J = 9.0 Hz, 2H), 8.02 (s, 1H), 7.60 (d, J = 8.7 Hz, 1H), 7.17 (s, 1H), 6.80 (d, J = 9.0 Hz, 2H), 6.74 (d, J = 8.8 Hz, 1H), 3.90 (s, 3H), 3.41 (t, J = 5.1 Hz, 4H), 3.26 (t, J = 6.6 Hz, 2H), 2.96 (t, J = 6.6 Hz, 2H), 2.66 (t, J = 5.0 Hz, 4H). ^{13}C NMR (100 MHz, Chloroform-*d*) δ 162.60, 154.57, 141.32, 138.94, 135.33, 126.70, 125.92, 113.01, 111.62, 53.79, 52.68, 52.49, 48.59, 47.04 ppm. MS (ESI, *m/z*): 422.2[M+H]$^+$.

*4.1.58. N-(6-methoxypyridin-3-yl)-2-(4-(pyrimidin-2-yl)piperazin-1-yl) ethane-1-sulfonamide (**10k**)*

Gray solid in 34.53% yield; mp 111.8–113.5 °C; ^{1}H NMR (500 MHz, Chloroform-*d*) δ 8.29 (d, J = 4.8 Hz, 2H), 8.04 (d, J = 2.8 Hz, 1H), 7.60 (dd, J = 8.8, 2.8 Hz, 1H), 6.73 (d, J = 8.8 Hz, 1H), 6.50 (t, J = 4.8 Hz, 1H), 3.89 (s, 3H), 3.84 (t, J = 5.1 Hz, 4H), 3.27 (t, J = 6.6 Hz, 2H), 2.96 (t, J = 6.6 Hz, 2H), 2.59 (t, J = 5.1 Hz, 4H). ^{13}C NMR (100 MHz, Chloroform-*d*) δ 162.49, 161.58, 157.81, 141.38, 135.23, 126.89, 111.52, 110.40, 53.80, 53.08, 52.71, 48.48, 43.56 ppm. MS (ESI, *m/z*): 379.2[M+H]$^+$.

*4.1.59. 2-(4-(4-methoxybenzyl)piperazin-1-yl)-N-(6-methoxypyridin-3-yl)ethane-1-sulfonamide (**10l**)*

Yellow gum in 26.63% yield; ^{1}H NMR (400 MHz, DMSO-d_6) δ 9.62 (s, 1H), 8.02 (d, J = 2.7 Hz, 1H), 7.57 (dd, J = 8.8, 2.8 Hz, 1H), 7.17 (d, J = 8.5 Hz, 2H), 6.84 (dd, J = 17.4, 8.7 Hz, 3H), 3.82 (s, 3H), 3.72 (s, 3H), 3.21–3.14 (m, 2H), 2.70–2.64 (m, 2H), 2.31 (d, J = 22.5 Hz, 7H). ^{13}C NMR (100 MHz, Chloroform-*d*) δ 162.34, 158.91, 141.20, 135.27, 130.46, 129.43, 127.08, 113.73, 111.43, 62.17, 55.32, 53.77, 53.00, 52.81, 52.51, 48.36 ppm. MS (ESI, *m/z*): 421.2[M+H]$^+$.

*4.1.60. 2-(4-benzylpiperazin-1-yl)-N-(naphthalen-1-yl)ethane-1-sulfonamide (**10m**)*

Brown solid in 84.30% yield; mp 89.0–90.0 °C; ^{1}H NMR (400 MHz, Chloroform-*d*) δ 8.13–8.07 (m, 1H), 7.88–7.83 (m, 1H), 7.72 (d, J = 8.2 Hz, 1H), 7.59 (d, J = 7.3 Hz, 1H), 7.55–7.48 (m, 2H), 7.45–7.39 (m, 1H), 7.31–7.19 (m, 5H), 3.36 (s, 2H), 3.33 (t, J = 6.5 Hz, 2H), 2.92 (t, J = 6.5 Hz, 2H), 2.41 (d, J = 59.1 Hz, 8H). ^{13}C NMR (100 MHz, Chloroform-*d*) δ 137.62, 134.52, 131.86, 129.24, 128.77, 128.65, 128.35, 127.29, 126.79, 126.70, 126.54, 125.75, 122.06, 120.87, 62.82, 53.06, 52.71, 52.67, 48.94 ppm. MS (ESI, *m/z*): 410.2[M+H]$^+$.

*4.1.61. N-(naphthalen-1-yl)-2-(4-(3-nitrobenzyl)piperazin-1-yl)ethane-1-sulfonamide (**10n**)*

Yellow solid in 48.65% yield; mp 105.1–106.8 °C; ^{1}H NMR (400 MHz, Chloroform-*d*) δ 8.15–8.04 (m, 3H), 7.88 (dd, J = 6.7, 2.4 Hz, 1H), 7.74 (d, J = 8.3 Hz, 1H), 7.57 (ddt, J = 12.4, 9.8, 6.6 Hz, 4H), 7.44 (t, J = 7.8 Hz, 2H), 3.45 (s, 2H), 3.37 (t, J = 6.5 Hz, 2H), 2.96 (t, J = 6.5 Hz, 2H), 2.43 (d, J = 69.2 Hz, 8H). ^{13}C NMR (100 MHz, Chloroform-*d*) δ 148.41, 140.40, 135.02, 134.52, 131.87, 129.27, 128.69, 126.82, 126.73, 126.56, 125.77, 123.72, 122.36, 122.00, 120.88, 61.75, 53.01, 52.68, 52.56, 48.96 ppm. MS (ESI, *m/z*): 455.2[M+H]$^+$.

*4.1.62. N-(naphthalen-1-yl)-2-(4-(4-nitrobenzyl)piperazin-1-yl)ethane-1-sulfonamide (**10o**)*

Brown solid in 79.04% yield; mp 104.7–106.7 °C; ^{1}H NMR (400 MHz, Chloroform-*d*) δ 8.12 (dd, J = 9.1, 2.9 Hz, 3H), 7.87 (dd, J = 6.7, 2.5 Hz, 1H), 7.73 (d, J = 8.2 Hz, 1H), 7.64–7.48 (m, 3H), 7.44 (d, J = 7.9 Hz, 1H), 7.40 (d, J = 8.6 Hz, 2H), 3.44 (s, 2H), 3.36 (t, J = 6.6 Hz, 2H), 2.94 (t, J = 6.6 Hz, 2H), 2.41 (d, J = 66.8 Hz, 8H). ^{13}C NMR (100 MHz, Chloroform-*d*) δ 147.25, 145.92, 134.52, 131.83, 129.51, 128.72, 128.69, 126.81, 126.77, 126.55, 125.77, 123.60, 121.98, 120.96, 61.86, 53.02, 52.77, 52.55, 48.98 ppm. MS (ESI, *m/z*): 455.2[M+H]$^+$.

*4.1.63. N-(naphthalen-1-yl)-2-(4-(4-nitrophenyl)piperazin-1-yl)ethane-1-sulfonamide (**10p**)*

Yellow solid in 29.87% yield; mp 224.8–225.1 °C; ^{1}H NMR (400 MHz, DMSO-d_6) δ 9.82 (s, 1H), 8.29 (d, J = 8.3 Hz, 1H), 8.03 (d, J = 9.4 Hz, 2H), 7.95 (d, J = 7.8 Hz, 1H), 7.84 (d, J = 7.8 Hz, 1H), 7.54 (dq, J = 15.3, 8.2, 7.5 Hz, 4H), 6.99 (d, J = 9.4 Hz, 2H), 3.41–3.36 (m, 7H), 2.85–2.76 (m, 2H), 2.48 (t, J = 5.0 Hz, 3H). ^{13}C NMR (100 MHz, DMSO-d_6) δ 155.14, 137.38, 134.48, 133.34, 129.79, 128.57, 126.93, 126.84, 126.78, 126.26, 126.18, 123.79, 123.11, 113.12, 52.39, 52.00, 49.78, 46.62 ppm. MS (ESI, *m/z*): 441.2[M+H]$^+$.

*4.1.64. N-(naphthalen-1-yl)-2-(4-(pyrimidin-2-yl)piperazin-1-yl)ethane-1-sulfonamide (**10q**)*

Green solid in 89.21% yield; mp 135.1–136.4 °C; ^{1}H NMR (400 MHz, Chloroform-*d*) δ 8.27 (d, J = 4.7 Hz, 2H), 8.10 (d, J = 8.2 Hz, 1H), 7.86 (d, J = 7.8 Hz, 1H), 7.74 (d, J = 8.2 Hz, 1H), 7.63 (d, J = 7.3 Hz, 1H), 7.59–7.40 (m, 3H), 6.47 (t, J = 4.8 Hz, 1H), 3.69 (t, J = 5.1 Hz, 4H), 3.40 (t, J = 6.7 Hz, 2H), 2.96 (t, J = 6.7 Hz, 2H), 2.53–2.45 (m, 4H). ^{13}C NMR (100 MHz, Chloroform-*d*) δ 161.48, 157.77, 134.48, 131.74, 128.78, 128.69, 126.97, 126.92, 126.58, 125.74, 121.81, 121.42, 110.19, 52.91, 52.60, 49.17, 43.38 ppm. MS (ESI, *m/z*): 398.2[M+H]$^+$.

*4.1.65. 2-(4-(4-methoxybenzyl)piperazin-1-yl)-N-(naphthalen-1-yl) ethane-1-sulfonamide (**10r**)*

Brown gum in 77.21% yield; ^{1}H NMR (400 MHz, DMSO-d_6) δ 9.75 (s, 1H), 8.27 (d, J = 7.8 Hz, 1H), 7.95 (d, J = 7.5 Hz, 1H), 7.82 (d, J = 7.0 Hz, 1H), 7.61–7.45 (m, 4H), 7.15 (d, J = 8.4 Hz, 2H), 6.85 (d, J = 8.3 Hz,

2H), 3.72 (s, 3H), 3.27 (d, $J = 7.5$ Hz, 2H), 2.75–2.68 (m, 2H), 2.29 (d, $J = 33.0$ Hz, 8H). ^{13}C NMR (100 MHz, Chloroform-*d*) δ 158.89, 134.51, 131.96, 130.51, 129.54, 128.89, 128.61, 126.81, 126.77, 126.54, 125.77, 122.22, 121.25, 113.71, 62.18, 55.35, 55.32, 52.93, 52.53, 52.47, 49.03 ppm. MS (ESI, *m/z*): 440.2$[M+H]^+$.

4.1.66. N-(5-((4-(2-(N-(naphthalen-1-yl)sulfamoyl)ethyl)piperazin-1-yl) methyl)thiazol-2-yl)acetamide (**10s**)

Brown solid in 3.55% yield; ^{1}H NMR (400 MHz, Chloroform-*d*) δ 12.19 (d, $J = 8.3$ Hz, 1H), 11.86 (d, $J = 7.5$ Hz, 1H), 11.74 (d, $J = 8.3$ Hz, 1H), 11.58–11.46 (m, 3H), 11.45–11.39 (m, 1H), 11.15 (s, 1H), 9.42 (s, 3H), 7.35–7.28 (m, 3H), 6.84–6.76 (m, 2H), 6.61 (s, 2H), 6.39 (s, 8H). ^{13}C NMR (100 MHz, DMSO-d_6) δ 168.69, 158.38, 136.25, 134.47, 133.26, 129.81, 128.56, 126.96, 126.77, 126.23, 123.79, 123.15, 53.83, 52.77, 52.42, 52.05, 49.74, 22.93 ppm. MS (ESI, *m/z*): 474.2$[M+H]^+$.

4.1.67. 2-(4-benzylpiperazin-1-yl)-N-(quinolin-6-yl)ethane-1-sulfonamide (**10t**)

Brown gum in 63.78% yield; ^{1}H NMR (400 MHz, Chloroform-*d*) δ 8.84 (d, $J = 3.9$ Hz, 1H), 8.07 (dd, $J = 11.9$, 8.5 Hz, 2H), 7.74 (d, $J = 2.5$ Hz, 1H), 7.46 (dd, $J = 9.0$, 2.5 Hz, 1H), 7.39 (dd, $J = 8.3$, 4.3 Hz, 1H), 7.34–7.21 (m, 5H), 4.85–4.38 (m, 2H), 3.51 (s, 2H), 3.32 (t, $J = 6.4$ Hz, 2H), 2.93 (t, $J = 6.4$ Hz, 2H), 2.49 (d, $J = 17.1$ Hz, 8H). ^{13}C NMR (100 MHz, Chloroform-*d*) δ 149.63, 145.50, 137.37, 135.83, 135.48, 130.87, 129.30, 128.92, 128.36, 127.35, 123.85, 121.96, 115.85, 62.82, 52.95, 52.73, 52.41, 48.63 ppm. MS (ESI, *m/z*): 411.2$[M+H]^+$.

4.1.68. 2-(4-(3-nitrobenzyl)piperazin-1-yl)-N-(quinolin-6-yl)ethane-1-sulfonamide (**10u**)

Brown solid in 71.07% yield; mp 99.9–101.9 °C; ^{1}H NMR (400 MHz, Chloroform-*d*) δ 8.84 (dd, $J = 4.3$, 1.7 Hz, 1H), 8.16 (t, $J = 2.0$ Hz, 1H), 8.12–8.04 (m, 3H), 7.76 (d, $J = 2.5$ Hz, 1H), 7.62 (d, $J = 7.6$ Hz, 1H), 7.54 (dd, $J = 9.0$, 2.5 Hz, 1H), 7.46 (t, $J = 7.9$ Hz, 1H), 7.40 (dd, $J = 8.3$, 4.2 Hz, 1H), 3.71 (s, 1H), 3.55 (s, 2H), 3.37 (t, $J = 6.7$ Hz, 2H), 2.95 (q, $J = 6.7$, 5.7 Hz, 2H), 2.47 (d, $J = 19.6$ Hz, 8H). ^{13}C NMR (100 MHz, Chloroform-*d*) δ 149.83, 148.48, 145.69, 140.31, 135.73, 135.20, 134.99, 131.08, 129.33, 128.91, 123.74, 123.71, 122.44, 122.03, 115.97, 61.82, 53.04, 52.90, 52.59, 48.53 ppm. MS (ESI, *m/z*): 456.2$[M+H]^+$.

4.1.69. 2-(4-(4-nitrobenzyl)piperazin-1-yl)-N-(quinolin-6-yl)ethane-1-sulfonamide (**10v**)

Brown solid in quantitive yield; mp 113.4–115.3 °C; ^{1}H NMR (400 MHz, Chloroform-*d*) δ 8.87 (dd, $J = 4.2$, 1.7 Hz, 1H), 8.22–8.14 (m, 2H), 8.14–8.05 (m, 2H), 7.75 (d, $J = 2.5$ Hz, 1H), 7.53–7.48 (m, 2H), 7.46 (dd, $J = 9.0$, 2.5 Hz, 1H), 7.42 (dd, $J = 8.3$, 4.2 Hz, 1H), 3.61 (s, 2H), 3.32 (t, $J = 6.2$ Hz, 2H), 2.97 (t, $J = 6.2$ Hz, 2H), 2.54 (d, $J = 22.6$ Hz, 8H). ^{13}C NMR (100 MHz, Chloroform-*d*) δ 149.88, 147.33, 145.81, 135.70, 135.14, 131.12, 129.50, 128.91, 123.74, 123.68, 122.04, 116.02, 61.95, 53.08, 53.01, 52.63, 48.51 ppm. MS (ESI, *m/z*): 456.2$[M+H]^+$.

4.1.70. 2-(4-(4-nitrophenyl)piperazin-1-yl)-N-(quinolin-6-yl)ethane-1-sulfonamide (**10w**)

Brown solid in 90.42% yield; mp 207.6–208.5 °C; ^{1}H NMR (400 MHz, DMSO-d_6) δ 10.51–9.90 (m, 1H), 8.79 (d, $J = 5.4$ Hz, 1H), 8.30 (d, $J = 7.8$ Hz, 1H), 8.00 (t, $J = 9.8$ Hz, 3H), 7.74 (d, $J = 2.7$ Hz, 1H), 7.62 (dd, $J = 8.8$, 2.5 Hz, 1H), 7.49 (dd, $J = 8.3$, 4.2 Hz, 1H), 6.96 (d, $J = 9.4$ Hz, 2H), 3.45 (t, $J = 7.1$ Hz, 2H), 3.30 (t, $J = 5.1$ Hz, 5H), 2.78 (t, $J = 7.1$ Hz, 2H), 2.44 (t, $J = 5.1$ Hz, 4H). ^{13}C NMR (100 MHz, DMSO-d_6) δ 155.10, 149.76, 145.26, 137.36, 136.95, 135.92, 130.77, 128.95, 126.17, 123.82, 122.46, 114.72, 113.09, 52.36, 52.02, 48.62, 46.56 ppm. MS (ESI, *m/z*): 442.2$[M+H]^+$.

4.1.71. 2-(4-(pyrimidin-2-yl)piperazin-1-yl)-N-(quinolin-6-yl)ethane-1-sulfonamide (**10x**)

Yellow gum in quantitive yield; ^{1}H NMR (400 MHz, Chloroform-*d*) δ 8.85 (dd, $J = 4.3$, 1.7 Hz, 1H), 8.29 (d, $J = 4.8$ Hz, 2H), 8.09 (dd, $J = 11.8$, 8.9 Hz, 2H), 7.76 (d, $J = 2.5$ Hz, 1H), 7.54 (dd, $J = 9.0$, 2.5 Hz, 1H), 7.40 (dd, $J = 8.3$, 4.2 Hz, 1H), 6.50 (t, $J = 4.8$ Hz, 1H), 3.80 (t, $J = 5.1$ Hz, 4H), 3.40 (t, $J = 6.6$ Hz, 2H), 2.96 (t, $J = 6.6$ Hz, 2H), 2.51 (t, $J = 5.1$ Hz, 4H). ^{13}C NMR (100 MHz, Chloroform-*d*) δ 161.46, 157.78, 149.68, 145.48, 135.86, 135.44, 130.94, 128.93, 123.70, 122.02, 115.73, 110.27, 52.94, 52.54, 48.67, 43.46 ppm. MS (ESI, *m/z*): 399.2$[M+H]^+$.

4.1.72. 2-(4-(4-methoxybenzyl)piperazin-1-yl)-N-(quinolin-6-yl)ethane-1-sulfonamide (**10y**)

Brown gum in 73.06% yield; ^{1}H NMR (400 MHz, Chloroform-*d*) δ 8.86 (dd, $J = 4.2$, 1.7 Hz, 1H), 8.13–8.03 (m, 2H), 7.73 (d, $J = 2.5$ Hz, 1H), 7.43 (ddd, $J = 18.5$, 8.6, 3.4 Hz, 2H), 7.25–7.17 (m, 2H), 6.91–6.82 (m, 2H), 3.80 (s, 3H), 3.50 (s, 2H), 3.30 (t, $J = 6.2$ Hz, 2H), 2.96 (t, $J = 6.2$ Hz, 2H), 2.54 (d, $J = 23.6$ Hz, 8H). ^{13}C NMR (100 MHz, Chloroform-*d*) δ 158.91, 149.60, 145.51, 135.80, 135.55, 130.84, 130.52, 129.29, 128.91, 123.84, 121.93, 115.78, 113.72, 62.17, 55.31, 52.90, 52.60, 52.36, 48.60 ppm. MS (ESI, *m/z*): 441.2$[M+H]^+$.

4.1.73. General preparation of compound **11a-11g**

Intermediate compound **7k** was dissolved in acetonitrile at 85 °C. Then potassium carbonate, potassium iodine, and different piperazines were added and reflux was performed overnight. After reaction completion, the solution was vacuumed to remove acetonitrile and water was added, followed by extraction with DCM. The products were then purified by flash column (DCM: MeOH = 20: 1) to obtain the desired compounds.

4.1.74. 4-(4-benzylpiperazin-1-yl)-3-nitro-N-(pyridin-2-ylmethyl) benzenesulfonamide (**11a**)

Orange gum in 69.40% yield; ^{1}H NMR (400 MHz, Chloroform-*d*) δ 8.43 (s, 1H), 8.16 (s, 1H), 7.80 (d, $J = 8.9$ Hz, 1H), 7.60 (s, 1H), 7.32 (s, 4H), 7.28 (d, $J = 7.0$ Hz, 1H), 7.19–7.10 (m, 2H), 7.02 (d, $J = 8.8$ Hz, 1H), 6.34 (s, 1H), 4.28 (s, 2H), 3.56 (s, 2H), 3.15 (d, $J = 5.3$ Hz, 4H), 2.58 (s, 4H). ^{13}C NMR (100 MHz, Chloroform-*d*) δ 154.52, 149.07, 148.07, 139.47, 137.55, 136.85, 131.75, 130.23, 129.15, 128.35, 127.32, 126.51, 122.72, 122.10, 119.97, 62.83, 52.46, 50.68, 47.41 ppm. MS (ESI, *m/z*): 468.2$[M+H]^+$.

4.1.75. 3-nitro-4-(4-(3-nitrobenzyl)piperazin-1-yl)-N-(pyridin-2-ylmethyl) benzenesulfonamide (**11b**)

Orange solid in 40.41% yield; mp 90.2–90.8 °C; ^{1}H NMR (400 MHz, Chloroform-*d*) δ 8.44 (s, 1H), 8.22 (d, $J = 20.7$ Hz, 2H), 8.14 (d, $J = 8.3$ Hz, 1H), 7.84 (d, $J = 8.8$ Hz, 1H), 7.67 (d, $J = 7.7$ Hz, 1H), 7.65–7.57 (m, 1H), 7.51 (s, 1H), 7.16 (d, $J = 7.9$ Hz, 2H), 7.04 (d, $J = 8.8$ Hz, 1H), 6.12 (s, 1H), 4.29 (s, 2H), 3.66 (s, 2H), 3.18 (s, 4H), 2.62 (s, 4H). ^{13}C NMR (100 MHz, Chloroform-*d*) δ 154.40, 149.07, 148.48, 148.03, 140.18, 139.71, 136.89, 134.95, 131.84, 130.66, 129.33, 126.45, 123.69, 122.76, 122.46, 122.10, 120.12, 61.77, 52.49, 50.67, 47.38 ppm. HRMS (ESI, *m/z*): calcd. for $C_{23}H_{25}N_6O_6S[M+H]^+$, 513.1556; found, 513.1545.

4.1.76. 3-nitro-4-(4-(4-nitrobenzyl)piperazin-1-yl)-N-(pyridin-2-ylmethyl) benzenesulfonamide (**11c**)

Orange solid in 91.82% yield; mp 89.9–90.2 °C; ^{1}H NMR (400 MHz, Chloroform-*d*) δ 8.43 (d, $J = 4.9$ Hz, 1H), 8.23–8.15 (m, 3H), 7.83 (dd, $J = 8.9$, 2.3 Hz, 1H), 7.61 (t, $J = 7.6$ Hz, 1H), 7.53 (d, $J = 8.4$ Hz, 2H), 7.16 (dd, $J = 14.1$, 8.0 Hz, 2H), 7.04 (d, $J = 8.8$ Hz, 1H), 6.29 (d, $J = 6.2$ Hz, 1H), 4.28 (d, $J = 2.8$ Hz, 2H), 3.67 (s, 2H), 3.21–3.14 (m, 4H), 2.64–2.57 (m, 4H). ^{13}C NMR (100 MHz, Chloroform-*d*) δ 154.56, 149.06, 147.99, 147.27, 145.71, 139.59, 136.94, 131.82, 130.66, 129.51, 126.40, 123.61, 122.76, 122.22, 120.18, 61.85, 52.55, 50.66, 47.46 ppm. HRMS

(ESI, *m/z*): calcd. for $C_{23}H_{25}N_6O_6S[M+H]^+$, 513.1556; found, 513.1545.

4.1.77. 3-nitro-4-(4-(4-nitrophenyl)piperazin-1-yl)-N-(pyridin-2-ylmethyl)benzenesulfonamide (**11d**)

Yellow solid in 95.72% yield; mp 129.7–130.9 °C; ^{1}H NMR (400 MHz, DMSO-d_6) δ 8.39 (d, J = 4.8 Hz, 1H), 8.35 (s, 1H), 8.10 (dd, J = 5.9, 3.4 Hz, 3H), 7.82 (dd, J = 8.9, 2.3 Hz, 1H), 7.34 (dd, J = 21.0, 8.4 Hz, 2H), 7.20 (dd, J = 7.5, 4.9 Hz, 1H), 7.00 (d, J = 9.3 Hz, 2H), 4.13 (s, 2H), 3.68 (dd, J = 6.9, 3.7 Hz, 4H), 3.40 (dd, J = 6.7, 3.8 Hz, 4H). ^{13}C NMR (100 MHz, Chloroform-*d*) δ 154.28, 154.22, 148.99, 147.61, 139.55, 139.08, 137.18, 132.07, 131.23, 126.66, 126.08, 122.95, 122.26, 119.64, 112.68, 49.81, 47.31, 46.42 ppm. MS (ESI, *m/z*): 499.1 $[M+H]^+$.

4.1.78. 3-nitro-N-(pyridin-2-ylmethyl)-4-(4-(pyrimidin-2-yl)piperazin-1-yl)benzenesulfonamide (**11e**)

Orange solid in 70.51% yield; mp 169.0–169.9 °C; ^{1}H NMR (400 MHz, DMSO-d_6) δ 8.41 (d, J = 4.7 Hz, 2H), 8.38 (dt, J = 5.8, 3.0 Hz, 2H), 8.09 (d, J = 2.3 Hz, 1H), 7.81 (dd, J = 8.9, 2.3 Hz, 1H), 7.68 (td, J = 7.7, 1.8 Hz, 1H), 7.38 (d, J = 9.0 Hz, 1H), 7.31 (d, J = 7.8 Hz, 1H), 7.20 (dd, J = 7.6, 4.8 Hz, 1H), 6.69 (t, J = 4.7 Hz, 1H), 4.14 (s, 2H), 3.91–3.84 (m, 4H), 3.29–3.21 (m, 4H). ^{13}C NMR (100 MHz, Chloroform-*d*) δ 161.49, 157.88, 154.49, 149.05, 148.20, 139.48, 137.09, 131.93, 130.70, 126.67, 122.87, 122.29, 119.97, 110.61, 50.41, 47.42, 43.21 ppm. MS (ESI, *m/z*): 456.2$[M+H]^+$.

4.1.79. 4-(4-(4-methoxybenzyl)piperazin-1-yl)-3-nitro-N-(pyridin-2-ylmethyl)benzenesulfonamide(**11f**)

Orange gum in 58.62% yield; ^{1}H NMR (400 MHz, Chloroform-*d*) δ 8.47–8.40 (m, 1H), 8.18 (d, J = 2.3 Hz, 1H), 7.81 (dd, J = 8.8, 2.3 Hz, 1H), 7.60 (td, J = 7.7, 1.8 Hz, 1H), 7.23 (d, J = 8.4 Hz, 4H), 7.14 (t, J = 7.0 Hz, 2H), 7.02 (d, J = 8.9 Hz, 1H), 6.91–6.83 (m, 2H), 5.99 (t, J = 5.3 Hz, 1H), 4.28 (d, J = 5.1 Hz, 2H), 3.81 (s, 3H), 3.50 (s, 2H), 3.19–3.11 (m, 4H), 2.60–2.52 (m, 4H). ^{13}C NMR (100 MHz, Chloroform-*d*) δ 158.90, 154.50, 149.07, 148.06, 139.40, 136.87, 131.74, 130.35, 130.17, 129.48, 126.49, 122.73, 122.14, 119.98, 113.71, 62.19, 55.27, 52.33, 50.66, 47.42 ppm. MS (ESI, *m/z*): 498.2$[M+H]^+$.

4.1.80. N-(5-((4-(2-nitro-4-(N-(pyridin-2-ylmethyl)sulfamoyl)phenyl)piperazin-1-yl)methyl)thiazol-2-yl)acetamide (**11g**)

Yellow solid in 13.93% yield; mp 212.9–213.9 °C; ^{1}H NMR (400 MHz, DMSO-d_6) δ 11.99 (s, 1H), 8.39–8.30 (m, 2H), 8.03 (d, J = 2.3 Hz, 1H), 7.77 (dd, J = 8.9, 2.3 Hz, 1H), 7.67 (td, J = 7.7, 1.8 Hz, 1H), 7.34–7.27 (m, 3H), 7.19 (dd, J = 7.6, 4.9 Hz, 1H), 4.12 (d, J = 5.8 Hz, 2H), 3.71 (s, 2H), 3.13 (t, J = 4.7 Hz, 4H), 2.52 (s, 4H), 2.12 (s, 3H). ^{13}C NMR (100 MHz, DMSO-d_6) δ 168.72, 157.10, 149.24, 137.09, 136.62, 131.97, 128.33, 125.93, 122.90, 122.36, 121.44, 53.72, 52.15, 50.74, 48.47, 22.94 ppm. MS (ESI, *m/z*): 532.2$[M+H]^+$.

4.2. Cells and biological reagents

Mouse IL-6 and TNF-α ELISA kits were obtained from eBioscience Inc. (San Diego, CA, USA). Lipopolysaccharide (LPS) was purchased from Sigma-Aldrich (St Louis, MO, USA). J774A.1 cells were obtained from ATCC Inc. and cultured in Dulbecco's modified Eagle's medium (DMEM) media (Gibco, Eggenstein, Germany) supplemented with 10% fetal bovine serum (FBS, Hyclone, Logan, UT), 100 mU/mL penicillin, and 100 mg/mL streptomycin. Cells were incubated at 37 °C under a 5% CO_2 atmosphere. The compounds were added to the culture medium in DMSO solution with the final 0.1% concentration of DMSO.

4.3. Detection of TNF-a and IL-6 secretion

TNF-α and IL-6 concentrations in culture media or animal samples were determined by ELISA according to the manufacturer's instructions (Bioscience, San Diego, CA). The amount of TNF-α or IL-6 was normalized to the protein concentration of each sample.

4.4. Assessment of cytotoxicity of designed compounds

To assess the safety of compounds, they were tested for their cytotoxicity in the J774A.1 cell line by MTT assay at a concentration of 10 μM. After 24 h, the cells' survival rates were measured in relation to the chemicals that had been administered.

4.5. Western blotting

J774A.1 macrophages were treated with different concentrations of **11d** or vehicle for 2 h. After being challenged with 0.5 μg/mL LPS for 15 min, cells were collected and lysed with RIPA lysis buffer containing protease and phosphatase inhibitor. Total protein samples were separated by 12% SDS-PAGE and electro-transferred to a 0.45 nm PVDF membrane. Membranes were blocked with 3% BSA in TBST buffer for 1 h at room temperature. Each membrane was incubated with specific primary antibodies against p-p65 (Cell Signaling #3033), Histone H3 (Proteintech #17168-1-AP), IκB-α (Cell Signaling #4812), and GAPDH (Cell Signaling #5174) at 4 °C for 16 h. Immunoreactive bands were then incubated with secondary horseradish peroxidase-conjugated (HRP) antibodies for 1 h at room temperature. The HRP signal was detected using an enhanced chemiluminescence reagent. The density of the immunoreactive bands was analyzed using ImageJ software (NIH, Bethesda, MD, USA).

4.6. Immunofluorescence

J774A.1 cells were cultured in the glass coverslips in 6-well plates. Macrophages were treated with or without **11d** for 2 h and then challenged with 0.5 μg/mL LPS for 15 min. The coverslips were fixed with 4% paraformaldehyde, following permeabilized with 0.1% Triton X-100 and blocked with 3% BSA in PBST buffer for 30 min. The cells were then incubated sequentially with a p65 (Cell Signaling #8242) antibody overnight at 4 °C. FITC-labeled secondary antibody was incubated with cells for 3 h at room temperature. The nucleus was stained with the DAPI and cell images were obtained using a ZEISS Axio Vert.A1 microscope.

4.7. LPS-induced model of acute lung injury

Male C57BL/6 mice weighing 18–22 g were purchased from the Animal Center of Wenzhou Medical University (Wenzhou, China). Mice were acclimatized at a constant room temperature with a 12:12 h light-dark cycle and provided with standard chow and water. The mice used in this study were treated following the Guide for Care and Use of Laboratory Animals of the National Institutes of Health. The animals were adapted to the laboratory environment for 7 days before initiating studies. The present study was approved by Wenzhou Medical College Animal Policy and Welfare Committee.

Mice were randomly divided into three groups: (1) control (n = 8); (2) LPS (n = 8); (3) LPS+**11d** (n = 8). Mice were treated by intragastric administration with **11d** compounds, at a dose of 20 mg/kg, 30 min before being challenged with LPS intratracheally (5 mg/kg). Control animals received 0.9% saline (NaCl). After 6 h of the LPS challenge, mice were euthanized with ketamine.BALF, blood, and lung tissues were collected for subsequent analysis.

4.8. Lung wet/dry (W/D) ratios

Pulmonary edema was evaluated by the lung wet/dry weight ratio. The middle lobe of the right lung tissue was collected, and the wet weight was documented. Then, lung tissues were heated in a constant thermostatic oven at 65 °C for 72 h and the dry weight was recorded. The ratio of wet/dry lung weight was reported.

4.9. BALF analysis

The collected BALF samples were centrifuged at 1000 rpm for 10 min at 4 °C, supernatant was collected and used for protein concentration detection and determination of cytokine levels. The cell pellet was re-suspended in 50 μL of PBS and the total number of cells in BALF was counted.

4.10. Histopathologic examination of tissues

The superior lobe of the right lung tissues was fixed in a 4% para-formaldehyde solution, embedded in paraffin, and sectioned in 5 μm slices. After dehydration, sections were stained with hematoxylin and eosin (H&E) using a standard protocol and observed with a Nikon Eclipse E800 microscope (Nikon, Tokyo, Japan).

4.11. Real-time quantitative PCR

The total RNA of cells and lung tissue were isolated using an RNA extraction kit (Invitrogen, Carlsbad, CA) according to the instruction given by the manufacturer. The reverse transcription and quantitative PCR were performed via a two-step M-MLV Platinum SYBR Green PCR SuperMix-UDG kit (Invitrogen, Carlsbad, CA). An Eppendorf Mastercycler ep realplex detection system (Eppendorf, Hamburg, Germany) was used for qPCR analysis. The primers for TNF-α and IL-6 genes were obtained from Thermo Fisher. Transcript levels were normalized by the amount of β-actin.

4.12. DSS-induced ulcerative colitis

Male C57BL/6 mice weighing 18–22 g were purchased from the Animal Center of Hangzhou Medical College (Hangzhou, China). Mice were acclimatized at a constant room temperature with a 12:12 h light-dark cycle and provided with standard chow and water. The mice used in this study were treated following the Guide for Care and Use of Laboratory Animals of the National Institutes of Health. The animals were adapted to the laboratory environment for 7 days before initiating studies. The present study was approved by the Wenzhou Institute, University of Chinese Academy of Sciences Animal Policy and Welfare Committee.

Mice were randomly divided into three groups: (1) control (n = 5); (2) DSS (n = 5); (3) DSS+**11d** (n = 5). Mice in the DSS group and DSS+**11d** group received 2.5% DSS for 7 days, the control group received normal water during the experiment. Mice in DSS+**11d** received 5 mg/kg **11d** in a mixture of DMSO/2.5% CMC-Na solution every day for 10 days. At the end of the experiment, the colon and spleen were removed and measured, the blood was collected.

4.13. Pharmacokinetic study

Male SD rats weighing 180–220 g were purchased from the Animal Center of Hangzhou Medical College (Hangzhou, China). Rats were fasted overnight with free access to water and predosed blood samples were withdrawn. The rats used in this study were treated following the Guide for Care and Use of Laboratory Animals of the National Institutes of Health. The present study was approved by Hangzhou Medical College Animal Policy and Welfare Committee.

Rats were randomly divided into two groups to receive intravenous or oral administration of **11d**. The compound **11d** was given to rats at a dose of 10 mg/kg orally or 1 mg/kg intravenously after being dissolved in a mixture of PEG400 and saline (50/50, v/v). After administration, the blood samples were collected from the caudal vein into heparinized centrifugation tubes at 5 min, 10 min, 15 min, 30 min, 1 h, 2 h, 3 h, 4 h, 5 h, 6 h, 8 h, 10 h, 12 h, and 24 h after dosing, and the blood samples of the oral administration rats were collected at 15 min, 30 min, 1 h, 2 h, 3 h, 4 h, 5 h, 6 h, 8 h, 10 h, 12 h, and 24 h after dosing (200 μL of blood each time). After centrifuging the tubes at 3000 rpm for 10 min at 4 °C to separate the plasma and stored at −20 °C in the freezer. Subsequently, 200 μL of an internal standard in acetonitrile was added to 40 μL of the plasma in order to extract the compound. Following 10 min of vortex mixing, the mixture was centrifuged at 8000 rpm for the same amount of time. The concentration of each animal was calculated using the LC-MS/MS Triple Quad 6500 plus system (SCIEX, USA). The PK solver software was used to determine the pharmacokinetic parameters.

4.14. Statistical analysis

The differences between different groups were analyzed by the student's t-test or ANOVA multiple comparisons in GraphPad Prism 6.0 (GraphPad, San Diego, CA). Data are expressed as the mean ± standard error of three independent experiments. $p < 0.05$ was considered significant (*), and $p < 0.01$ was considered very significant (**).

Declaration of competing interest

The authors declare that they have no known competing financial interests or personal relationships that could have appeared to influence the work reported in this paper.

Data availability

Data will be made available on request.

Acknowledgments

This study was funded in part with the funds provided by Zhejiang Provincial Key Scientific Project (2021C03041), the National Natural Science Funding of China (82273791, 21961142009), Research Fund from the University of Chinese Academy of Sciences (WIUCASQD2020016) and Scientific Research Starting Foundation in Wenzhou Medical University (QTJ21013).

Appendix A. Supplementary data

Supplementary data to this article can be found online at https://doi.org/10.1016/j.ejmech.2023.115706.

References

[1] M.L. Tang, H. Li, J.F. Ning, X. Shen, X. Sun, Discovery of first-in-class TAK1-MKK3 protein-protein interaction (PPI) inhibitor (R)-STU104 for the treatment of ulcerative colitis through modulating TNF-alpha production, J. Med. Chem. 65 (2022) 6690–6709.
[2] Y.W. Wang, Y.H. Wu, J.Z. Zhang, J.H. Tang, R.P. Fan, F. Li, B.Y. Yu, J.P. Kou, Y. Y. Zhang, Ruscogenin attenuates particulate matter-induced acute lung injury in mice via protecting pulmonary endothelial barrier and inhibiting TLR4 signaling pathway, Acta Pharmacol. Sin. 42 (2021) 726–734.
[3] M.M. Gouda, Y.P. Bhandary, Acute lung injury: IL-17A-Mediated inflammatory pathway and its regulation by curcumin, Inflammation 42 (2019) 1160–1169.
[4] M. Menk, E. Estenssoro, S.K. Sahetya, A.S. Neto, P. Sinha, A.S. Slutsky, C. Summers, T. Yoshida, T. Bein, N.D. Ferguson, Current and evolving standards of care for patients with ARDS, Intensive Care Med. 46 (2020) 2157–2167.
[5] M. Zoulikha, Q. Xiao, G.F. Boafo, M.A. Sallam, Z. Chen, W. He, Pulmonary delivery of siRNA against acute lung injury/acute respiratory distress syndrome, Acta Pharm. Sin. B 12 (2) (2022) 600–620.
[6] P. Toner, D.F. McAuley, M. Shyamsundar, Aspirin as a potential treatment in sepsis or acute respiratory distress syndrome, Crit. Care 19 (2015) 374.
[7] R.E. Abdulnour, T. Gunderson, I. Barkas, J.Y. Timmons, C. Barnig, M. Gong, D. J. Kor, O. Gajic, D. Talmor, R.E. Carter, B.D. Levy, Early intravascular events are associated with development of acute respiratory distress syndrome. A substudy of the LIPS-A clinical trial, Am. J. Respir. Crit. Care Med. 197 (2018) 1575–1585.
[8] U. Hamid, A. Krasnodembskaya, M. Fitzgerald, M. Shyamsundar, A. Kissenpfennig, C. Scott, E. Lefrancais, M.R. Looney, R. Verghis, J. Scott, A.J. Simpson, J. McNamee, D.F. McAuley, C.M. O'Kane, Aspirin reduces lipopolysaccharide-induced pulmonary inflammation in human models of ARDS, Thorax 72 (2017) 971–980.
[9] G.R. Bernard, A.P. Wheeler, J.A. Russell, R. Schein, W.R. Summer, K.P. Steinberg, W.J. Fulkerson, P.E. Wright, B.W. Christman, W.D. Dupont, S.B. Higgins, B. B. Swindell, The effects of ibuprofen on the physiology and survival of patients

with sepsis. The Ibuprofen in Sepsis Study Group, N. Engl. J. Med. 336 (1997) 912–918.
[10] R. Ungaro, S. Mehandru, P.B. Allen, L. Peyrin-Biroulet, J.F. Colombel, Ulcerative colitis, Lancet 389 (2017) 1756–1770.
[11] X. Yuan, Y. Chen, M. Tang, Y. Wei, M. Shi, Y. Yang, Y. Zhou, T. Yang, J. Liu, K. Liu, D. Deng, C. Zhang, L. Chen, Discovery of potent and selective receptor-interacting serine/threonine protein kinase 2 (RIPK2) inhibitors for the treatment of inflammatory bowel diseases (IBDs), J. Med. Chem. 65 (2022) 9312–9327.
[12] A. Kolodziejska-Sawerska, A. Rychlik, A. Depta, M. Wdowiak, M. Nowicki, M. Kander, Cytokines in canine inflammatory bowel disease, Pol. J. Vet. Sci. 16 (2013) 165–171.
[13] M.F. Neurath, Cytokines in inflammatory bowel disease, Nat. Rev. Immunol. 14 (2014) 329–342.
[14] S. Xiao, W. Zhang, H. Chen, B. Fang, Y. Qiu, X. Chen, L. Chen, S. Shu, Y. Zhang, Y. Zhao, Z. Liu, G. Liang, Design, synthesis, and structure-activity relationships of 2-benzylidene-1-indanone derivatives as anti-inflammatory agents for treatment of acute lung injury, Drug Des. Dev. Ther. 12 (2018) 887–899.
[15] C. Ding, H. Chen, B. Liang, M. Jiao, G. Liang, A. Zhang, Biomimetic synthesis of the natural product salviadione and its hybrids: discovery of tissue-specific anti-inflammatory agents for acute lung injury, Chem. Sci. 10 (2019) 4667–4672.
[16] S. Mukhopadhyay, J.R. Hoidal, T.K. Mukherjee, Role of TNFalpha in pulmonary pathophysiology, Respir. Res. 7 (2006) 125.
[17] X. Liang, Y. Xie, X. Liu, H. Xu, H. Ren, S. Tang, Q. Liu, M. Huang, X. Shao, C. Li, Y. Zhou, M. Geng, Z. Xie, H. Liu, Discovery of novel imidazo[4,5-c]quinoline derivatives to treat inflammatory bowel disease (IBD) by inhibiting multiple proinflammatory signaling pathways and restoring intestinal homeostasis, J. Med. Chem. 65 (2022) 11949–11969.
[18] A. Noeparast, E. Teugels, P. Giron, G. Verschelden, S. De Brakeleer, L. Decoster, J. De Greve, Non-V600 BRAF mutations recurrently found in lung cancer predict sensitivity to the combination of Trametinib and Dabrafenib, Oncotarget 8 (2017) 60094–60108.
[19] G. Gentilcore, G. Madonna, N. Mozzillo, A. Ribas, A. Cossu, G. Palmieri, P. A. Ascierto, Effect of dabrafenib on melanoma cell lines harbouring the BRAF (V600D/R) mutations, BMC Cancer 13 (2013) 17.
[20] S. Viswanathan, B.D. Hammock, J.W. Newman, P. Meerarani, M. Toborek, B. Hennig, Involvement of CYP 2C9 in mediating the proinflammatory effects of linoleic acid in vascular endothelial cells, J. Am. Coll. Nutr. 22 (2003) 502–510.
[21] M.A. Olson, M.S. Lee, T.L. Kissner, S. Alam, D.S. Waugh, K.U. Saikh, Discovery of small molecule inhibitors of MyD88-dependent signaling pathways using a computational screen, Sci. Rep. 5 (2015), 14246.
[22] A.T. Ulusoy, E. Kalyoncuoglu, A. Reis, Z.C. Cehreli, Antibacterial effect of N-acetylcysteine and taurolidine on planktonic and biofilm forms of Enterococcus faecalis, Dent. Traumatol. 32 (2016) 212–218.
[23] W. Zhao, L. Jia, H.J. Yang, X. Xue, W.X. Xu, J.Q. Cai, R.J. Guo, C.C. Cao, Taurine enhances the protective effect of Dexmedetomidine on sepsis-induced acute lung injury via balancing the immunological system, Biomed. Pharmacother. 103 (2018) 1362–1368.
[24] B.M. Egan, H. Abdih, C.J. Kelly, C. Condron, D.J. Bouchier-Hayes, Effect of intravenous taurine on endotoxin-induced acute lung injury in sheep, Eur. J. Surg. 167 (2001) 575–580.
[25] H. Abdih, C.J. Kelly, D. Bouchier-Hayes, M. Barry, S. Kearns, Taurine prevents interleukin-2-induced acute lung injury in rats, Eur. Surg. Res. 32 (2000) 347–352.
[26] M. Giris, B. Depboylu, S. Dogru-Abbasoglu, Y. Erbil, V. Olgac, H. Alis, G. Aykac-Toker, M. Uysal, Effect of taurine on oxidative stress and apoptosis-related protein expression in trinitrobenzene sulphonic acid-induced colitis, Clin. Exp. Immunol. 152 (2008) 102–110.
[27] L. Chen, H. Chen, P. Chen, W. Zhang, C. Wu, C. Sun, W. Luo, L. Zheng, Z. Liu, G. Liang, Development of 2-amino-4-phenylthiazole analogues to disrupt myeloid differentiation factor 88 and prevent inflammatory responses in acute lung injury, Eur. J. Med. Chem. 161 (2019) 22–38.
[28] L. Chen, Y. Jin, H. Chen, C. Sun, W. Fu, L. Zheng, M. Lu, P. Chen, G. Chen, Y. Zhang, Z. Liu, Y. Wang, Z. Song, G. Liang, Discovery of caffeic acid phenethyl ester derivatives as novel myeloid differentiation protein 2 inhibitors for treatment of acute lung injury, Eur. J. Med. Chem. 143 (2018) 361–375.
[29] Z. Liu, L. Chen, P. Yu, Y. Zhang, B. Fang, C. Wu, W. Luo, X. Chen, C. Li, G. Liang, Discovery of 3-(Indol-5-yl)-indazole derivatives as novel myeloid differentiation protein 2/Toll-like receptor 4 antagonists for treatment of acute lung injury, J. Med. Chem. 62 (2019) 5453–5469.
[30] G. Chen, Y. Zhang, X. Liu, Q. Fang, Z. Wang, L. Fu, Z. Liu, Y. Wang, Y. Zhao, X. Li, G. Liang, Discovery of a new inhibitor of myeloid differentiation 2 from cinnamamide derivatives with anti-inflammatory activity in sepsis and acute lung injury, J. Med. Chem. 59 (2016) 2436–2451.
[31] J. Qian, X. Chen, S. Shu, W. Zhang, B. Fang, X. Chen, Y. Zhao, Z. Liu, G. Liang, Design and synthesis novel di-carbonyl analogs of curcumin (DACs) act as potent anti-inflammatory agents against LPS-induced acute lung injury (ALI), Eur. J. Med. Chem. 167 (2019) 414–425.
[32] T. Chen, Y. Wei, G. Zhu, H. Zhao, X. Zhang, Design, synthesis and structure-activity relationship studies of 4-indole-2-arylaminopyrimidine derivatives as anti-inflammatory agents for acute lung injury, Eur. J. Med. Chem. 225 (2021), 113766.
[33] L.Z. Chen, W.W. Sun, L. Bo, J.Q. Wang, C. Xiu, W.J. Tang, J.B. Shi, H.P. Zhou, X. H. Liu, New arylpyrazoline-coumarins: synthesis and anti-inflammatory activity, Eur. J. Med. Chem. 138 (2017) 170–181.
[34] S. Wirtz, V. Popp, M. Kindermann, K. Gerlach, B. Weigmann, S. Fichtner-Feigl, M. F. Neurath, Chemically induced mouse models of acute and chronic intestinal inflammation, Nat. Protoc. 12 (2017) 1295–1309.